

WeedNet: A Foundation Model-Based Global-to-Local AI Approach for Real-Time Weed Species Identification and Classification

Yanben Shen^{1†}, Timilehin T. Ayanlade^{3†}, Venkata Naresh Boddepalli¹, Mojdeh Saadati⁵, Ashlyn Rairdin¹, Zi K. Deng⁴, Muhammad Arbab Arshad³, Aditya Balu³, Daren Mueller², Asheesh K Singh¹, Wesley Everman¹, Nirav Merchant⁴, Baskar Ganapathysubramanian³, Meaghan Anderson¹, Soumik Sarkar^{3,*}, and Arti Singh^{1,*}

¹Department of Agronomy, Iowa State University, Iowa, USA.

²Department of Plant Pathology, Entomology and Microbiology, Iowa State University, Iowa, USA

³Department of Mechanical Engineering, Iowa State University, Iowa, USA.

⁴Data Science Institute, University of Arizona, Arizona, USA

⁵Department of Computer Science, Iowa State University, Iowa, USA.

*Address correspondence to: arti@iastate.edu, soumiks@iastate.edu

†These authors contributed equally to this work.

Abstract

Early identification of weeds is essential for effective management and control, and there is growing interest in automating the process using computer vision techniques coupled with artificial intelligence (AI) methods. However, challenges associated with training AI-based weed identification models, such as limited expert-verified data and complexity and variability in morphological features, have hindered progress. To address these issues, we present WeedNet, the first global-scale weed identification model capable of recognizing an extensive set of weed species, including noxious and invasive plant species. WeedNet is an end-to-end real-time weed identification pipeline and uses self-supervised learning, fine-tuning, and enhanced trustworthiness strategies. WeedNet achieved 91.02% accuracy across 1,593 weed species, with 41% species achieving 100% accuracy. Using a fine-tuning strategy and a Global-to-Local approach, the local Iowa WeedNet model achieved an overall accuracy of 97.38% for 85 Iowa weeds, most classes exceeded a 90% mean accuracy per class. Testing across intra-species dissimilarity (different developmental stages) and inter-species similarity (look-alike species) suggests that diversity in the images collected, spanning all the growth stages and distinguishable plant characteristics, is crucial in driving model performance. The generalizability and adaptability of the Global

WeedNet model enable it to function as a foundational model, with the Global-to-Local strategy allowing fine-tuning for region-specific weed communities. Additional validation of drone- and ground-rover-based images highlights the potential of WeedNet for integration into robotic platforms. Furthermore, integration with AI for conversational use provides intelligent agricultural and ecological conservation consulting tools for farmers, agronomists, researchers, land managers, and government agencies across diverse landscapes.

1 Introduction

Weeds have adapted to natural and human-modified environments, which leads to competition with cultivated crops for essential resources such as water, nutrients, light, and space, significantly affecting crop yields [1]. In the United States and Canada, the competition from weeds caused an average loss of \$26.7 billion in maize (*Zea mays* L.) from 2007 to 2013 [2], while wheat (*Triticum aestivum* L.) produces losses averaging \$2.19 billion for winter wheat and \$1.14 billion for spring wheat during the same period [3]. The dry bean (*Phaseolus vulgaris* L.) faced an average loss of \$622.2 million between 2007 and 2016 due to weed infestations[4], demonstrating the extensive economic impact of weeds on crop productivity.

Accurate identification of weeds is a crucial initial step in effective integrated weed management [5]. An important consideration is to correctly classify and categorize weed species. Weeds can be categorized according to the plant life cycle into annual, biennial, or perennial weeds; based on morphology into grasses, broad leaves, sedges and others; based on habitat into aquatic, terrestrial, and parasitic weeds; based on control method into herbicide-susceptible or herbicide-resistant weeds; on economic or agricultural impact into noxious weeds or crop-specific weeds and based on origin into native, introduced, or invasive weeds.

Invasive weed species pose a significant threat not only to agriculture but also to natural ecosystems. These species, which are not native to the environments they invade, can lead to the extinction of native plants, reduce biodiversity, and permanently alter habitats [6]. For example, leafy spurge (*Euphorbia esula*) is a highly invasive weed that reproduces through seed and vegetative structures. Its presence significantly reduces the species richness and, in some cases, native species can be eliminated [7]. Palmer amaranth (*Amaranthus palmeri*) is one of the most economically damaging weeds in corn, cotton and soybean production. Even when established in June or July, this weed exhibits intense competition with crops. It can continue to flower under the canopy of the crop for an extended period, resulting in a significant accumulation of biomass and a depletion of resources within the cropping systems [8]. However, the ecological impact of these invasive species is often realized only after they have become widespread, making early detection and classification critical for effective management [9].

The traditional method of manual weed identification is time-consuming and labor-intensive, involving visual inspection in the field, making it less effective for quick real-time weed management decisions, especially on large-scale farms. In production agriculture, where a herbicide-tolerant crop is grown, a blanket spray with an appropriate herbicide can somewhat circumvent the need for detailed weed scouting; however, if used throughout the season, it is an undesirable practice, as

it causes propagation of herbicide-tolerant weed species and long-term production challenges [10]. Resistance to herbicides is a prevalent problem, with an average of five new cases emerging annually between 1990 and 2015 [11]. For example, Palmer amaranth and common waterhemp (*Amaranthus tuberculatus*), two similar species of the Amaranth family, show different herbicide resistance profiles, highlighting the need for an accurate identification [12, 13].

Correct identification in an early growth stage is crucial for implementing targeted control measures, optimizing weed management costs, and preventing the spread of weed populations [14, 15]. Misidentification of weed species can lead to ineffective control methods, exacerbating infestations [16, 17]. During scouting, environmental factors such as lighting and soil conditions can affect visibility, while the spatial variability of the weed distributions makes the comprehensive coverage complex [18, 19]. Timing is crucial, as scouting must be done early and frequently for optimal weed management and control [20]. Detecting new invasive species in diverse landscapes adds to the challenges of weed identification and its management [21]. In addition, achieving high accuracy in manual weed mapping and density estimation for large fields is problematic in itself. This highlighting the need to integrate manual techniques with emerging technologies such as AI-based detection systems [22], particularly edge devices such as smartphones [23, 24], unmanned aerial vehicles (UAVs) [25], and ground robots [26] to improve accuracy and efficiency in early identification and management of weeds.

Artificial intelligence (AI) is rapidly emerging as a transformative technology that aids farmers and scouts in the timely identification and mitigation of plant diseases [27–29], insects [30, 31], and weeds [22, 32]. Image-based phenotyping has significantly advanced weed detection through non-destructive high-throughput methods for accurate plant classification and spatial distribution [33]. Drones and ground robots equipped with RGB, multispectral, and hyperspectral cameras have been used to automatically capture high-resolution field images, supporting the development of algorithms for automatic weed detection and mapping [34, 35], diseases [27–29], and insects [30, 31]. Satellite imagery combined with AI-driven analytics has also facilitated large-scale monitoring of weed infestation dynamics [36, 37]. Remote sensing technologies integrated with AI offer scalable and precise solutions for weed management in precision agriculture by enabling real-time species-level identification of weeds. A key challenge is developing AI models capable of distinguishing subtle differences between crops, weeds, and lookalike species under field conditions, which the PlantCLEF challenge addresses [38]. This global competition uses a dataset of 80,000 plant species to tackle issues associated with many classes, class imbalance, variable image data quality, and noisy field backgrounds. For example, PlantCLEF’s 2023 dataset included more than 1.2 million annotated images to train convolutional neural networks (CNN) for fine-grained identification. These advances improve the accuracy of AI-driven weed detection tools while minimizing false positives, bridging the gap between scalable data collection and actionable weed management strategies [39, 40].

Several challenges are associated with the automated identification of weeds in crop production scenarios. These challenges include (a) data, (b) model, (c) performance, and (d) deployment.

Data Challenge: The primary challenge in developing robust AI-based deep learning models for identifying weeds in agriculture is the limited quantity and quality of image-based datasets. Quantity concerns include the total number of images and the adequate representation of each

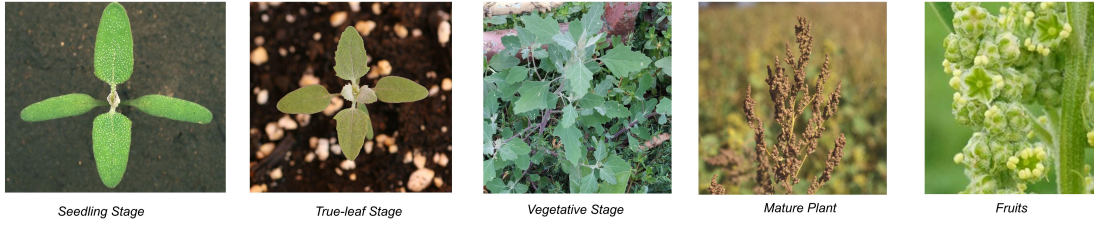
class. High-quality data must include diverse high-resolution images taken under varying conditions such as lighting, growth stages, soil types, and moisture levels. Previous studies have reviewed publicly available weed datasets [34, 41, 42] (see Supplementary Material S1). However, many contain images from controlled environments, such as greenhouses, lacking phenological variability of plants [43, 44]. In addition, these datasets often collect weed images from their local region, which reflects regional biases and makes it difficult to compile diverse datasets for comprehensive AI models. Expanding data set diversity is crucial to improve model generalization and performance. Citizen science platforms such as iNaturalist provide large-scale data collections throughout the world, offering research-grade photos with species-level identification [45]. An example of a research-grade observation shows the characteristics of the plant in the leaf blade, sheath, head, and seeds of green foxtail (*Setaria viridis*) [46]. Previous studies have compared the quality of research-grade iNaturalist observations with digitized herbarium specimens, finding a low misidentification rate between the two sources, which supports the utility of iNaturalist data [47]. However, there are concerns about class imbalance, as iNaturalist data often underrepresents rare or difficult-to-identify species and overrepresents common ones due to observer preferences and accessibility.

Model Challenge: Selecting the appropriate deep learning model for weed identification requires balancing model complexity, computational resources, data availability, and the need for high accuracy in real-world agricultural applications. Early attempts used hand-made features and traditional machine learning (ML) techniques such as support vector machines (SVM) and random forests (RF) to differentiate crops and weeds based on color, shape and texture descriptors [48–50]. However, these models struggled with variations in the morphology of the weeds and complex environmental conditions, limiting their applicability. Recent studies have used deep neural network architectures such as CNNs to improve accuracy in diverse field conditions. Pre-trained CNN architectures like ResNet-50, EfficientNet, and DenseNet have shown success in multiclass weed identification in cotton fields [51]. Graph-based deep learning models have also been developed for complex conditions [52]. Deep CNN-based models have been used to classify multiple weed species under various weather and sunlight conditions [53, 54]. Semi-supervised methods, such as semi-supervised generative adversarial networks (SGAN), have emerged to address the challenge of obtaining labeled data, achieving high accuracy with minimal labeled data [55]. SemiWeedNet integrates labeled and unlabeled images for weed segmentation and identification, improving the robustness of the model [56]. Despite these advancements, traditional deep learning models like CNNs face difficulties in generalizing and scaling due to insufficient data diversity and variability in training datasets [34, 57]. Recent models like transformers, built around attention mechanisms such as vision transformers (ViT), offer better scalability, precision, and efficiency for large-scale image classification tasks compared to CNNs [58]. ViTs capture global contextual relationships in images, making them effective for applications such as autonomous systems [59] and precision agriculture [60]. A significant challenge arises when weed identification models provide inaccurate predictions with high confidence, affecting user trust and system reliability [61, 62]. Misclassifying weeds and crops can lead to unintended crop removal or weed survival, adversely affecting yields and profitability. The inability to warn users of the uncertainty of the model in predicting weed species similar to the lookalike can erode confidence in AI applications. Environmental variability, such as different lighting conditions and soil types,

can cause inconsistent model performance and erode user confidence. Data bias from nonrepresentative training datasets can lead to unreliable predictions. The lack of explainability in complex "black box" models makes it difficult for users to trust their output, especially when errors occur [63].

Performance Challenge: The performance of weed identification models in real-world scenarios depends on their ability to accurately detect various weed species under variable field conditions, including common noxious, invasive, and look-alike species. Intra-species dissimilarity refers to individual differences within the same species (Figure 1) [38]. For example, common lambsquarters (*Chenopodium album*) show considerable intraspecific variation in leaf shape and size, influenced by environmental factors such as soil nutrients and water availability [64]. Horseweed (*Erigeron canadensis*) also exhibits distinct visual differences between its rosette and flowering stages, which complicates identification [65–67]. In contrast, inter-species similarity involves similarities between different species, including shared physical characteristics and ecological niches [68]. Morphological similarity occurs when two or more weed species resemble each other in leaf shape, growth habit, flower structure, or seeds [69] (Figure 2). For example, the amaranth species, such as red-root pigweed (*Amaranthus retroflexus*), Palmer amaranth, and common waterhemp, often co-exist in disturbed habitats, making differentiation difficult. Poisonous and non-poisonous species within the Apiaceae family (also known as the carrot family) share traits like pinnately divided leaves and umbel-shaped flower clusters, complicating identification [70]. Accurate identification is essential, as the wild parsnip (*Pastinaca sativa*) has a phototoxic sap that poses risks to public safety. In contrast, caraway (*Carum carvi*) and Golden Alexanders (*Zizia aurea*) have different ecological importance; Golden Alexanders is a beneficial native species and caraway is a useful culinary herb. Monocot species, such as yellow foxtail (*Setaria pumila*), green foxtail (*Setaria viridis*), and giant foxtail (*Setaria faberi*), require a close examination of morphological traits. Key identification features include the presence and distribution of hairs in leaf blades, the color and shape of the bristly seed heads, and the structure of the ligules and auricles for accurate identification [71] (Figure 2: Foxtail weeds).

Common lambsquarters (*Chenopodium album*)



Horseweed (*Erigeron canadensis*)



Figure 1: Examples of intra-species dissimilarity across developmental stages in common lambsquarters (*Chenopodium album*) and horseweed (*Erigeron canadensis*). The images show plant characteristics such as leaf shape, leaf margin, and change in plant morphology from seedling to fruiting stages. These variations within a single species across growth stages highlight the challenge for models to identify species consistently.

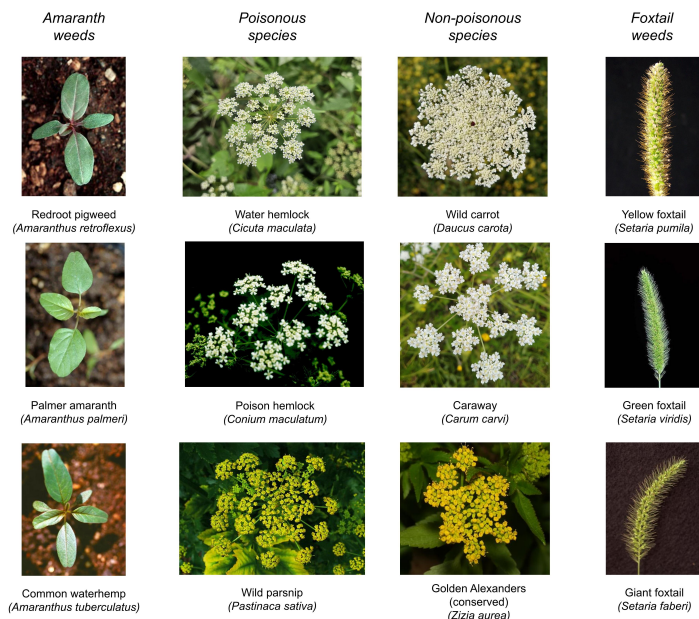


Figure 2: Examples illustrating inter-species similarity challenges among various weed groups. The figure includes morphologically similar species from amaranth weeds, poisonous and non-poisonous species within the Apiaceae family, and closely related foxtail species. Despite toxicity or ecological function differences, these species exhibit similar phenotypic features, complicating accurate field identification.

The National Invasive Species Information Center (NISIC) lists approximately 60 terrestrial invasive plant species, including trees, shrubs, vines, grasses, and herbaceous plants [6]. These invasive plants include trees, shrubs, vines, grasses, and herbaceous plants. Examples include giant hogweed (*Heracleum mantegazzianum*), purple loosestrife (*Lythrum salicaria*), purple starthistle (*Centaurea calcitrapa*), kudzu (*Pueraria montana*), garlic mustard (*Alliaria petiolata*), Japanese knotweed (*Reynoutria japonica*), Johnsongrass (*sorghum halepense*), mile-a-minute (*Persicaria perfoliata*), tree of heaven (*Ailanthus altissima*), common ivy (*Hedera helix*), common buckthorn (*Rhamnus cathartica*) and witchweed (*Striga asiatica*) (Supplementary Figure S1). Early detection is essential to prevent their establishment and spread, as they can outcompete native vegetation, reduce biodiversity, and disrupt ecosystems. These species cause significant ecological and economic damage by altering habitats and reducing crop productivity. For example, witchweed parasitizes cereal crops, leading to total yield loss in subsistence farms [72]. Fast-growing invaders such as kudzu and Japanese knotweed smother native vegetation, incurring billions in control costs [73, 74]. Herbicide-resistant weeds, such as Johnsongrass, common waterhemp, giant ragweed, and Palmer amaranth, complicate eradication and challenge existing management strategies [10, 75]. Several invasive weeds also host damaging insects, amplifying their agricultural impact. The tree of heaven supports the invasive pest spotted lanternfly (*Lycorma delicatula*), a pest of fruit trees and vines [76]; common buckthorn shelters soybean aphids [77]; Johnsongrass harbors sugarcane aphids and crop viruses [78]; common barberry (*Berberis vulgaris*) serves as an alternate host for black stem rust (*Puccinia graminis*), a

devastating disease of wheat, barley, and other small grains [79]. and the kudzu weed supports the invasive pest kudzu bug, which reduces soybean yields [80]. Rapid identification and management efforts informed by early detection protocols can mitigate their impacts and reduce long-term control costs [9].

Operational Challenge: The deployment of AI models to detect weeds poses significant computational challenges, as complex deep learning models require substantial computational resources [81]. An ongoing research challenge is to balance algorithm complexity with processing capacity for real-time field applications and optimize AI models for efficient processing on edge devices [82]. Integrating AI-based weed detection models into edge devices such as smartphones, rovers, and drones requires seamless integration for automated identification and real-time decision-making.

Integrating the weed identification model into a smartphone app provides a convenient tool for users to connect to the AI model for fast and accurate identification and take timely action for weed control. The traditional app works more like the conventional weed guide, which requires the user to select plant characteristics, such as plant type, color, and leaf shape [83]. In comparison, AI models use computer vision and are more convenient for giving automated results. During a five-year period, a weed specialist tested several smartphone apps for plant identification purposes [84]. The data set used included broadleaf, grassy, ornamental, and shrub species. The study emphasized that a simple process is key to user-friendliness and overall experience when using such tools. Among the tested applications, PictureThis delivered the highest performance, with an average accuracy of 73% [84]. However, these apps were designed primarily to identify general plant species rather than pest weed species for agricultural or ecological concerns.

These gaps motivate this research to develop a global model for weed identification for common noxious and invasive plant species that are considered weed species in production and non-production agriculture settings. A global model is trained on a large and diverse collection of plant images, such as those on platforms such as iNaturalist, using self-supervised learning (SSL). This model learns general visual patterns of a wide range of plant species from various regions, without relying on labeled data. Although the global model captures rich and transferable features for plant identification, it may not be specifically optimized for detecting or classifying agriculturally relevant weeds in a specific region or cropping system. A local model is trained exclusively on region-specific and expert-validated data sets focused on weeds that affect particular cropping systems or areas, for example, weeds that impact corn and soybean production in the Midwestern US. This model is highly accurate for the narrow task of identifying locally important weed species, but it may struggle with generalization to broader or unfamiliar contexts. Therefore, we used a global-to-local approach to fine-tune a pre-trained global model for weed species in Iowa, US, demonstrating its effectiveness even with limited local imagery [31]. This method starts with a broadly trained model and fine-tunes it using smaller, high-quality, expert-labeled datasets tailored to specific regions or crop systems. By combining the generalization strength of the global model with the precision of local data, this hybrid approach reliably identifies key weeds in targeted agricultural settings while reducing the need for extensive local annotation.

To address the above challenges in data quantity and quality, model generalization and performance, and deployment, this study presents WeedNet. This global-scale weed identification model

combines self-supervised learning with a global-to-local fine-tuning strategy [85]. Built using the ViT architecture [86], the foundation model (global model) was trained on a large-scale dataset derived from iNaturalist, capturing broad variability across weed species and environmental conditions. To improve relevance and accuracy in regional applications, the global model is fine-tuned using smaller, expert-validated local datasets [31, 87]. This transfer learning approach takes advantage of the generalizability of large models while requiring less data and computation, reducing overfitting on limited datasets [88]. By integrating citizen science data with expert labels, Weed-Net ensures reliable real-world performance. Its adaptability across platforms such as smartphones, drones, and ground rovers supports efficient, locally optimized weed detection for diverse agricultural environments and stakeholders worldwide.

2 Materials and Methods

2.1 Dataset

The image data set was obtained from iNaturalist, which consists of 257 million observations spanning five kingdoms, including approximately 172K plant species [89]. To obtain relevant weed images, we carefully curated the image dataset with invasive species profiles list (60 species, NISIC, USDA) [90], Midwest Invasive Plant Network (458 plant species in the US and Ontario, Canada) [91] and Bugwood images (1,916 plant species) [92] to filter it down to 1593 species categories of relevant plants, including crop species, crop-specific weeds, noxious weeds, invasive weeds, and weed species from across the world (Supplementary S2). We excluded species with fewer than 100 research-grade images in the iNaturalist dataset. The final data set comprises 14 million images, which were checked to ensure accurate species labels (Figure 3).

Data acquisition and transformation were performed using the Large Data Acquisition Workflow Template (LDAWT), a specialized software suite. This suite facilitates the download and query of the iNaturalist database, generating file manifests based on specified criteria. In addition, it optimizes manifest groupings to enhance download throughput and performance. Using a template-based approach, LDAWT transforms and organizes data during the download process, thereby minimizing the subsequent renaming and reorganization necessary for model training. These manifest files are then transmitted to TaskVine, a parallelized, distributed, and fault-resistant workflow manager, enabling concurrent asynchronous downloads from geographically diverse locations, including cloud virtual machines and high-performance computing (HPC) data transfer nodes. LDAWT aggregates the final output in a machine learning-ready format and deposits it into a shared cloud storage repository. LDAWT effectively utilizes available network bandwidth in a cooperative manner, this approach prevents denial of service to data providers such as iNaturalist while simultaneously transferring terabytes of data.

2.2 Model

2.2.1 Global Model - Pretraining and Finetuning Approach

Accurate machine learning models are based on the availability of annotated datasets, where each image is labeled with a corresponding category. However, large-scale data set annotation remains a significant bottleneck, especially when expert verification is required. To mitigate this challenge, we adopt a self-supervised learning approach (SSL) (Figure 3), which allows the model to learn meaningful representations without requiring labeled data. This enables effective feature learning that can be later fine-tuned using a smaller labeled dataset, improving model generalization and performance. We used twenty images per species from the iNaturalist data for testing and validation. Additionally, to comprehensively evaluate the accuracy of our model, we assessed performance on a diverse collection of public domain web images and images collected from our field test, representing different developmental stages of weed species. A total of 6,962 images were captured from April to November 2023 in corn, soybeans, mung beans, and field pea fields in Ames, Iowa, US, covering Iowa weed species at various stages of life using smartphones. The publicly available web images for the global weed species were sourced from government agencies, university extension programs, and academic repositories that excluded iNaturalists to assess identification challenges. Several thousand images were tested separately for four challenges in the Introduction section.

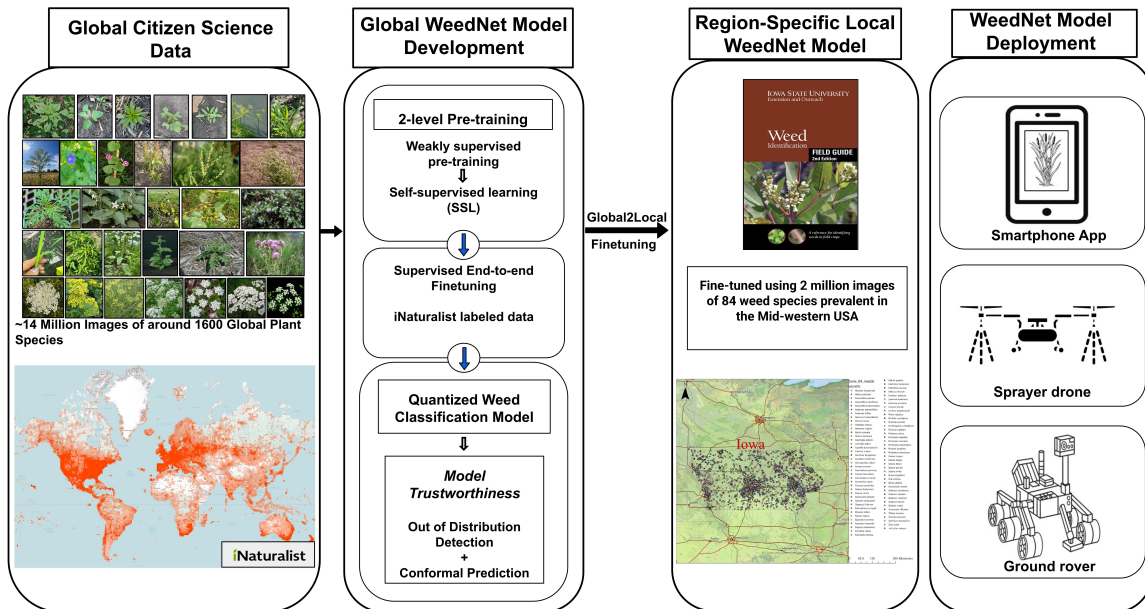


Figure 3: Overview of the Global Weed Model Development and Implementation. The Global Weed AI Model is trained on approximately 14 million images covering around 1600 plant species from the iNaturalist database. The end-to-end WeedNet pipeline was deployed on smartphones for real-time weed identification. The Global-to-Local approach enables fine-tuning on region-specific weed species using fewer images, reducing computational requirements while improving accuracy. Such local, region-specific lightweight models could identify weed images captured using robotic platforms such as UAVs and ground rovers, possibly deploying such models for high-throughput real-time weed identification.

SSL pretraining follows a pretrain-then-finetune paradigm, which has proven successful in various computer vision tasks, including image identification and object detection [31, 93, 94]. Instead of relying on supervised labels, SSL methods learn general-purpose visual representations by solving a pre-training task on large-scale unlabeled data. Early approaches focused on reconstruction-based objectives [95], alongside other techniques such as contrastive learning [96], and joint embedding methods [97, 98]. With the emergence of ViTs [99], reconstruction-based strategies have regained interest due to their simplicity and state-of-the-art performance [100, 101]. We conducted training experiments in CNN-based (RegNet) and Transformer-based (MAE) architectures to evaluate the performance and impact of pretraining, with the Transformer-based model outperforming the CNN-based model (see Supplementary Material S6).

In this work, we use the Masked Autoencoder (MAE) [101], a self-supervised learning strategy that has demonstrated superior performance in multiple transfer tasks [101–103] while maintaining computational efficiency (see Supplementary Material S4). Our pipeline involved multiple data preparation steps (see Supplementary Material S3) followed by two pre-training levels, an initial pre-training using a large-scale dataset of 3.5 billion images with Instagram hashtags, with the same methodology described in Mahajan et al. (2018)[94]. Then, 14 million unlabeled weed images

followed a subsequent pre-training. We performed end-to-end fine-tuning on 14 million labeled images (Table 1). We conducted extensive training experiments on multiple dataset sizes and model sizes to systematically assess the impact of SSL pre-training. The performance of the fine-tuned models was evaluated using standard identification metrics (top-1 and top-5 accuracy) to determine the effectiveness of our approach (see Supplementary Materials S7 and S8).

Table 1: Overview of the WeedNet model development pipeline and performance across eight development and evaluation processes. Stages 1 and 2 represent the self-supervised pretraining process using ViT-based Masked Autoencoders (MAE) on large-scale unlabeled datasets: 3.5 billion Instagram images and 14 million iNaturalist plant-related images. Stages 3 and 4 involve supervised fine-tuning using 14 million labeled iNaturalist weed images, whereas stage 4 involves the addition of expert datasets. The conformal prediction feature (Stage 5) was integrated to improve the model’s trustworthiness. Stages 6 and 7 demonstrate local model fine-tuning using 2M labeled regional weed data. Stage 8 involves the evaluation of the model on other open-source multiple expert-curated datasets under k-shot scenarios. Across the pipeline, SSL pretraining combined with fine-tuning strategies trained on citizen and expert data sources developed WeedNet and Global-to-local models.

Stage	Description	Data Source	Labels	Categories	Acc.	Gain
1	Pre-pretraining	~3.5B Instagram images	No	-	-	-
2	Pretraining	~14M iNat plant-related images	No	-	-	-
3	Finetuning (Global model)	~14M iNat weed images	Yes	1593	90.50	-
4	Finetuning (Global model + expert data)	~14.3M iNat + expert	Yes	1593	91.02	+0.52
5	Conformal prediction	ImageNet12, FaceMask, Weeds	Mixed	-	91.02	-
6	Finetuning (Local model)	~2M weed images	Yes	84	97.38	-
7	Local + expert data	~2M + 11k expert images	Yes	84	97.68	+0.30
8	K-shot evals	Various expert datasets	Yes	≤ 24	-	-

2.2.2 Global-to-local Finetuning

We adopt a hierarchical strategy to achieve accurate and local context-aware identification of weeds. This begins with leveraging the trained WeedNet model (global model) and implemented a global-to-local fine-tuning approach to develop a region-specific weed identification model for the Midwest US (Figure 3 and Table 1). This method began with a robust global model trained on 14 million images. Stages 1 and 2 represent the self-supervised pretraining process using ViT-based MAE on large-scale unlabeled datasets: 3.5 billion Instagram images and 14 million iNaturalist plant-

related images. Stages 3 and 4 involve supervised fine-tuning using 14 million labeled iNaturalist weed images, while Stage 4 consists of adding expert datasets. The conformal prediction feature (Stage 5) was integrated to improve the trustworthiness of the model. Stages 6 and 7 demonstrate local model fine-tuning using 2M labeled regional weed data. Stage 8 involves the evaluation of the model on other open-source multiple expert-curated datasets under k-shot scenarios. Across the pipeline, SSL pretraining combined with fine-tuning strategies trained on citizen and expert data sources developed WeedNet and Global-to-local models. We then fine-tuned this model using an expert-verified dataset of approximately 2 million images (Table 1), focusing on the 84 prevalent weed species affecting the Midwest corn and soybean cropping systems, as detailed in the Iowa State University Extension and Outreach Weed Identification Field Guide [104].

2.2.3 Improving Model Trustworthiness

Out of Distribution Detection - Two wrapper models, namely out-of-distribution (OOD) detection and conformal prediction, are incorporated into the model to enhance trustworthiness. OOD detection helps avoid misclassifying unfamiliar inputs as known classes, which leads to losing trustworthiness. OOD detection mitigates this by helping models recognize data that deviate from the training distribution, improving reliability [105–109]. The OOD algorithm assigns a confidence score that indicates how likely a test sample belongs to the training set; factors such as model architecture and class distribution influence its effectiveness. Saadati et al. [110] recently evaluated these factors and demonstrated that energy-based models (EBMs) [108] outperform alternatives on multiple performance metrics. This paper follows the experimental pipeline from [110].

In this paper, we selected EBM as the OOD algorithm and wrapped the algorithm around the trained classifier, following the same analysis procedure as [110]. For data preprocessing of model (EBM) training, we used the test set of an in-distribution weed dataset (ID), selecting five random samples from each of the 1593 classes. Three (60%) were used to train the EBM, and two (40%) were reserved to test the EBM. As OOD datasets, we used Human Face [111] and ImageNet [112]. Due to a slight discrepancy of 41 samples between the total ID and OOD dataset sizes, we randomly sampled from the in-distribution data to ensure that both sets were equal. Specifically, we used 4,860 images from the ImageNet 2012 subset (excluding weeds or insects), 3,059 images from the NoMask facemask recognition datasets for the OOD dataset. For the ID data set, we used 7,965 images from the weed test data, which includes five samples from each class.

Conformal Prediction - To increase the trustworthiness and accuracy of the prediction of the weed detection model, we incorporated the conformal prediction into the model. In cases where the model is uncertain about a prediction, it is more reliable to output a set of potential labels rather than a single one. Conformal prediction [113] supports this by generating sets of labels based on a confidence level α , ensuring that the true label is included with high probability. For our task, we considered the hyperparameter $\alpha = 0.95$. Our approach consisted of the following steps, using the same hyperparameter setting as in paper [114] while conserving the structure of the original algorithm [113]: First, we took eight random samples from each of 1593 classes from ID test data to create the conformal training set (4 images per class, 50%) and the conformal testing set (4 images

per class, 50%). Then, we pick a heuristic function, maximum softmax probability, to measure the conformal score for all images in the training set. We calculated the score for each data point in the conformal training set and then sorted all scores. For a given threshold α , the score value of $1 - \alpha$ of the data sets is more significant than that score, called this value \hat{q} . In the application phase, we compared the softmax value of all classes with \hat{q} , and if the value was higher, we included that class in the conformal set.

2.3 Model Performance

To evaluate the performance of the WeedNet model in intra-species dissimilarity, a subsample of 84 weed species that are important to Iowa were selected [104]. A set of web-sourced images for each selected weed species capturing early plant stages (seedling to 3 true leaves), vegetative stages, and reproductive stages was used to test the model’s performance. Due to limited image availability for particular species across all stages from the Internet, the number of images per species was standardized based on the least available stage, ensuring a consistent ratio among the three growth stages. To evaluate the model’s performance on inter-species similarity, the web image set included species previously reported as lookalike species into three categories: Grass family (5 species), Apiaceae family (11 species), and Amaranth family (8 species) [115–118]. The images of each species were collected using the same developmental stage-based strategy described above.

2.4 Model Deployment for Seamless Operation on Edge Devices

To evaluate the WeedNet on the deployment, we used weed images captured using UAVs and ground rovers during field experiments in 2024 in Ames, Iowa, US Image collection began three weeks after planting at the 2 to 3 true leaf stage, using UAVs and rovers to capture weeds at different growth stages in inter-row areas and field borders. A DJI Inspire 2 drone (*DJI, Shenzhen*) equipped with a Zenmuse X5S RGB camera captured aerial images at 15 m above ground level (AGL). A ground rover (*Farm-ng, California*) carrying a Insta360 Titan a VR 360 8K Camera (*Insta360, Shenzhen*) captured images at 1.5 m AGL while moving through interrows. The visual survey involved the identification of groundweeds, with geographic coordinates recorded using an Emlid Reach RS+ Real-time kinematic (RTK) positioning global navigation satellite system receiver. UAV images were stitched and preprocessed in Pix4D with a ground sampling distance of 0.1-0.12 cm/pixel. The final stitched field image was analyzed in ArcGIS Pro and validated against ground truth to assess the model’s accuracy.

The WeedNet model was evaluated in two distinct settings: (i) targeted identification of the same 15 specific weeds throughout the evaluation period and (ii) an untargeted (random) visual survey evaluating the presence of various weeds in the field on each survey date. A total of 425 annotated weed images from UAV images and 110 annotated weed images from rover images cover eight species from the early stage in August to the reproductive stage in September. The weed species included: common waterhemp, common lambsquarters, venice mallow (*Hibiscus trionum*), spotted spurge (*Euphorbia maculata*), common purslane (*Portulaca oleracea*), green carpetweed (*Mollugo verticillata*), yellow foxtail, and common groundcherry (*Physalis Longifolia*).

For integrating WeedNet into a smartphone app, the trained WeedNet model was deployed as a REST API using FastAPI, providing a lightweight interface for real-time predictions [119]. The backend processes input images and returns the predicted species and alternative candidates with confidence scores. The conformal prediction intervals, described in Section 2.2.3, are included to quantify uncertainty.

A user-friendly front-end application communicates with this API, enabling users to submit images and receive results (two-step process). The interface of the WeedNet app is shown below (Figure 4). To ensure system stability, requests are rate-limited to 30 calls per minute. Despite using CPU-based inference for cost efficiency, the pipeline delivers predictions within practical timeframes (typically under 3 seconds per image). The front and back ends are hosted on OpenShift as isolated microservices, ensuring modular maintenance.

Furthermore, the WeedNet model is integrated with a chatbot, resulting in PestIDBot. A large language model can combine WeedNet prediction with a retrieval-augmented generative model to create a comprehensive pest management decision support tool [119]. Such systems can leverage WeedNet’s identification capabilities to accurately determine weed species and then use this information to retrieve and communicate relevant management strategies through natural dialogue with users. Visual recognition and conversational AI integration create more accessible and practical tools for agricultural decision making. Caraway examples show that PestID provides identification, taxonomic classification of species, and works as a chatbot with the user (see Supplementary Materials S9 and S10).

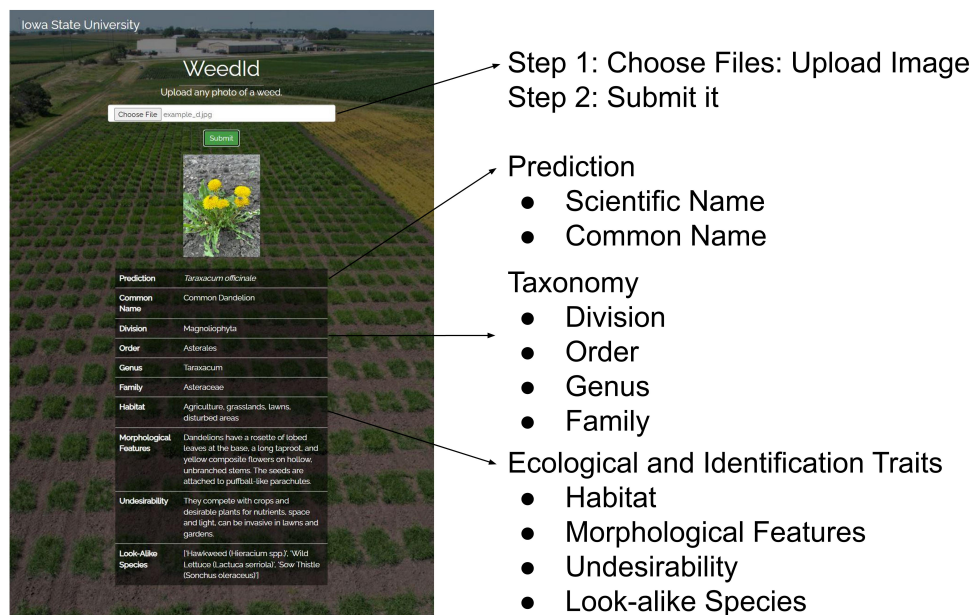


Figure 4: Example interface of the PestIDBot application on a common dandelion image. Users upload weed images for identification and return a prediction. The app also provides users with information on taxonomy, ecology, and identification traits.

2.5 Model Evaluation

Table 2 summarizes the testing approaches used to evaluate the Global model and its variants by fine-tuning. The model’s performance was also evaluated on specialized data sets, including intra-species dissimilarity, inter-species similarity, and UAV/Ground Rover images to assess its robustness in agricultural applications.

Table 2: Overview of Models Used to Evaluate Performance

Model Used to Test	Number of Species	Testing Image Dataset
Global model	1593	20 testing images per species
Global-to-Local model	84	20 testing images per species
Refined model	11	20 testing images per species
Global model	84	Web image dataset of intra-species dissimilarity
Global model	24	Web image dataset of inter-species similarity
Global model	8	UAV and Ground Rover images

The performance of the model was evaluated in the confusion matrix under four categories, including true positive (TP), false positive (FP), true negative (TN) and false negative (FN). TP represents the number of correct identification; FP represents the number of other species misclassified as this species; FN represents the number of this species misclassified as others. Macro Precision, Macro Recall, and Macro F1 score were calculated according to the confusion matrices to assess the model capability and effectiveness. n represents the total number of images.

$$\text{Accuracy} = \left(\sum_{i=1}^n TP_i \right) / n \quad (1)$$

$$\text{MacroPrecision} = \left(\sum_{i=1}^n \frac{TP_i}{TP_i + FP_i} \right) / n \quad (2)$$

$$\text{MacroRecall} = \left(\sum_{i=1}^n \frac{TP_i}{TP_i + FN_i} \right) / n \quad (3)$$

$$\text{MacroF1} = \left(\sum_{i=1}^n \frac{2TP_i}{2TP_i + FP_i + FN_i} \right) / n \quad (4)$$

3 Results

We organized the results to follow the four main challenges in developing and deploying an AI model for real-time weed identification and classification.

3.1 Data Challenges

3.1.1 Global Citizen Science Dataset

Citizen science data have become a valuable source for building ML models [31] and provide a broad range of images or data points from various geographical regions, increasing the diversity and scope of the data set [120]. In this study, we used an iNaturalist dataset that contains 1,593 weed classes and 813 genera with a total of ~ 14 M images, which contain a wide diversity of weed species worldwide. The species with the highest number of training images is common yarrow (*Achillea millefolium*) with 150,154 images, while common salt tree (*Caragana halodendron*) has the fewest (182 images). The median number of training images per species is 3,347, and only 11% of the species have fewer than 500 images. This large quantity and quality diverse dataset enables the deep learning model to capture intra- and inter-species variability, improving its ability to make accurate identifications across fields.

3.2 Model Challenges

3.2.1 Global WeedNet Model Development

Our top-performing model was developed through a multistage process: an initial pre-training campaign on a large out-of-domain dataset, i.e., non-weed dataset (3.5 billion Instagram hashtag images), followed by a second stage of SSL pre-training on the in-domain, i.e., weed dataset (iNaturalist), and concluding with supervised finetuning on labeled data (iNaturalist, + list of all other datasets used here) (Table 1). This model, termed WeedNet, achieved a classification accuracy of 91.02%. The histogram of accuracy for all 1593 categories of weed species shows that 41% of the species have 100% accuracy and 89.7% of the species have a test accuracy greater than 80% (Figure 5A). Furthermore, increasing the number of training images does not consistently lead to higher test accuracy. Among species with 100% accuracy, there is a wide range of training images, from 188 to 15,054 (Figure 5B).

Analyzing the misclassification results suggests that the low model performance is primarily due to look-alike features and data imbalance. The results of the 1,593 species model showed that 16 species had an accuracy below 20% (Supplementary Table S6). Among these sixteen species, most misidentifications occurred with other species of the same taxonomic family. For example, of 20 test images of animated oat (*Avena sterilis*), thirteen were incorrectly identified as wild oat (*Avena fatua*), a species within the same genus, indicating that the model struggled to distinguish species with similar phenological and morphological traits (Supplementary Figure S4 and Table S7). Furthermore, many misclassified images were misidentified as species with significantly more training data, suggesting that data imbalance and potential overfitting are also contributing factors. For example, northern dock (*Rumex longifolius*) achieved only 5% accuracy despite having 783 training images. Thirteen of its 20 test images were misclassified as curled dock (*Rumex crispus*), a species with 100% test accuracy and 32,739 training images (Supplementary Figure S5 and Table S8). This emphasizes the problem of training data imbalance in the foundation model and the need to collect an adequate image dataset for the prevalent regional weeds and training with the

global-to-local approach.

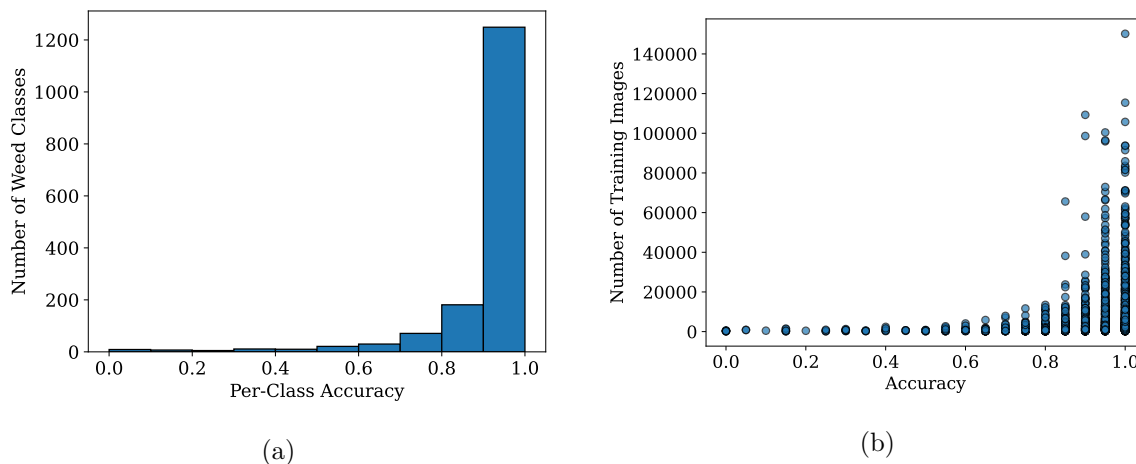


Figure 5: (a) Histogram showing the per-class accuracies across 1593 weed species. The plot reveals that nearly 90% of the classes achieve over 80% accuracy. (b) Scatter plot illustrating the relationship between prediction accuracy and the amount of training data for the model. Increasing the number of training images does not consistently lead to higher test accuracy. Some weed species with fewer training images often achieve high accuracy, showcasing the model’s ability to handle classes with limited data effectively. However, these classes struggle when species within the same family have significantly larger training datasets, leading to imbalanced performance.

3.2.2 Region-Specific Weed Identification through Global-to-Local Fine-Tuning

We apply a global-to-local approach to develop a regional weed identification model for the Midwestern US [121]. The local model focuses on the most prevalent weed species that affect agricultural practices, particularly those that affect the maize and soybean cropping systems, resulting in a subset of 84 weed species. The global-to-local fine-tuned model achieved an overall accuracy of 97.38%, with most classes exceeding 90% per class accuracy (Figure 6 A). However, eleven species: *Amaranthus palmeri*, *Cenchrus longispinus*, *Eleusine indica*, *Eriochloa villosa*, *Muhlenbergia schreberi*, *Persicaria maculosa*, *Persicaria pensylvanica*, *Setaria faber*, *Setaria pumila*, *Setaria viridis*, *Sorghum bicolor*, exhibited lower accuracies. To address this performance gap, we integrated expert-verified samples from various datasets [51, 54, 122, 123] specifically for low-performing species and fine-tuned the existing model (Figure 6B). The refined WeedNet local model (using the Global-to-Local approach), trained with expert-validated data, had an improved accuracy of 97.68% (Figure 6 C and Table1). According to conformal prediction, the eleven species that previously showed confusion in accurate identification had increased accuracy after adding expert-verified images. For example, a local model trained to identify 84 species using the iNaturalist dataset achieved 80% mean per class accuracy in detecting Palmer amaranth with 1,995 photos. Adding 1,331 more images increased this accuracy to 85%, enhancing prediction confidence and reducing uncertainty. This underscores the importance of supplementing iNaturalist data with expert-verified images for the low-accuracy weed species classes to minimize noise and strengthen model robustness for regional weed identification. Figure 6 highlights the effectiveness of incorporating curated datasets. Including expert-verified images

for confusing classes provides a scalable solution for weed management, enabling models to leverage large-scale citizen science data while ensuring high accuracy through targeted fine-tuning with expert-verified samples, even for local weeds.

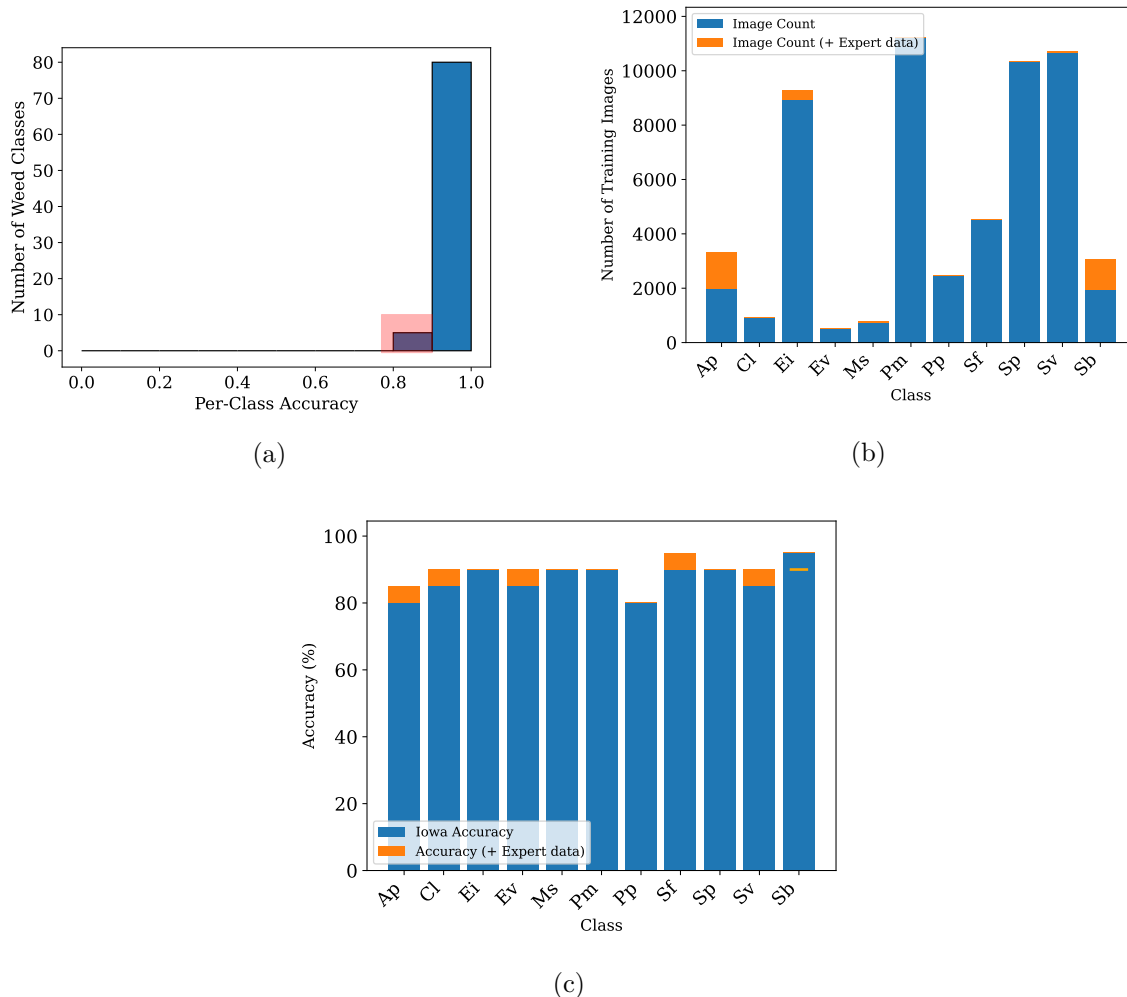


Figure 6: The figures of the global-to-local fine-tuned model (a) Histogram depicting per-class accuracies across 84 Midwestern U.S. weed species, with low-performing classes (accuracy below 90% or 0.9). (b) Bar plot showing the distribution of the number of images in low-performing species, including the count of expert-collected data for these classes. (c) Bar plot illustrating the accuracy improvement for low-performing species with expert data. The 11 Classes: Ap= *Amaranthus palmeri*, Cl= *Cenchrus longispinus*, Ei= *Eleusine indica*, Ev= *Eriochloa villosa*, Ms= *Muhlenbergia schreberi*, Pm= *Persicaria maculosa*, Pp= *Persicaria pennsylvanica*, Sf= *Setaria faberi*, Sp= *Setaria pumila*, Sv= *Setaria viridis*, Sb= *Sorghum bicolor*

After establishing success in developing a global-to-local model for the Midwest US using expert-verified image data set for low-sample-sized weed species (Figure 6), we additionally showcase the effectiveness of the SSL model and demonstrate that using a small number of samples ($k = 0, 10, 20$, and all) to fine-tune SSL pre-trained WeedNet can yield good accuracies in diverse locations. These

four datasets include the CottonWeed12 dataset [123], the CottonWeed15 dataset [51], the 2Seasons dataset [34], the DeepWeeds dataset [54] and the WeedsAI dataset [122], which were carefully curated and annotated by specialists, ensuring the accuracy of the labels. The 0-shot and 10-k-shot results in Table 3 demonstrate a significant increase in the model’s accuracy. The examples of the Midwest U.S. and four independent datasets suggest that SSL pretraining on a vast dataset, followed by fine-tuning on smaller, expert-verified datasets, produces the variant model for particular regions.

Table 3: Performance of weed datasets under zero-shot ($k=0$) and Few-shot ($k=10$, $k=20$) and full finetuning ($k=all$) settings. The top-1 identification accuracies for the experiments are reported. In the Zero-shot evaluation, 11, 5, and 15 classes are common with our 1593 dataset classes for CottonWeedDet12, DeepWeeds, and WeedsAI datasets, respectively. Details are provided in Supplementary S5

Dataset	Classes	k-shot Accuracy (%)			
		k=0	k=10	k=20	k=all
CottonWeedDet12 [123]	12	66.82	98.75	98.75	99.17
CottonWeedDet15 [51]	15	72.33	98.33	98.67	98.70
2Season [34]	8	65.62	100.00	100.00	100.00
DeepWeeds [54]	8	42.00	82.89	83.22	98.33
WeedsAI [122]	24	70.72	86.82	90.05	98.26

3.2.3 Out-of-Distribution Detection Analysis

We evaluated the performance of EBM on the trained weed model following the same procedure as [110, 114]. We evaluated the uncertainty quantification under the three performance measures of AUROC (area under the ROC curve), AURP (area under the precision recall diagram), and FPR95 (false positive rate at 95% true positive). The threshold for the OOD classifier is chosen based on the ROC curve as -8.2484 to have a maximum separation between the ID and OOD data (Figure 7); also, the hyperparameter T (temperature) is selected by hyperparameter tuning as 0.02. The results illustrate that the OOD classifier achieved an AUROC of 98.63, an AUPR of 97.8, an FPR95 of 0.026, and an accuracy of 95.20 % in detecting out-of-distribution data. The mapping of test data into energy can lead to a more significant distinction between ID and OOD data (Figure 7A).

3.2.4 Conformal Prediction Analysis

In this analysis, we set the hyperparameter α to 0.05, which led us to a threshold \hat{q} of 0.903 on the confidence score. Therefore, the algorithm includes a class name in the conformal prediction set if its confidence score, softmax value, is greater than $1 - \hat{q}$. The trained conformal prediction algorithm covered the correct label with an accuracy of 0.947. We illustrate an example of the performance of our trained conformal prediction in (Figure 7B).

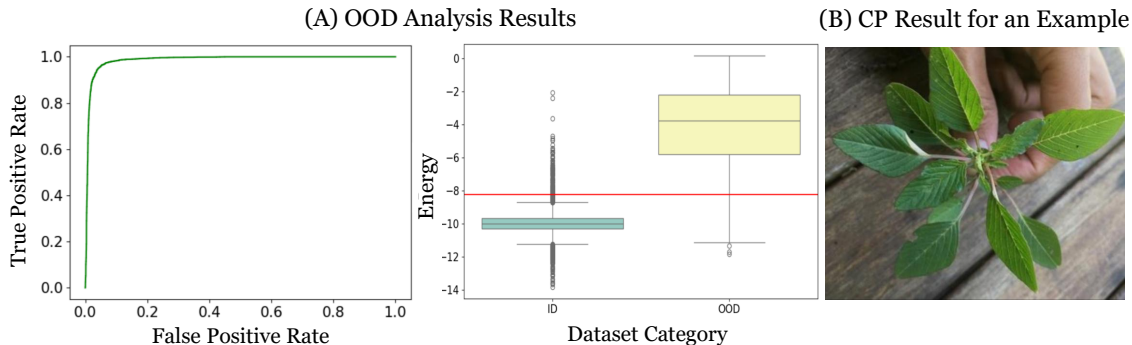


Figure 7: ROC curve over all possible threshold values. We chose a threshold value that provides the lowest FPR at 95% true positive rate (left). Box plot of energy values for in-distribution weed dataset (ID) and out-of-distribution (OOD) data. The red line is the threshold value used for separating ID and OOD data (center). Conformal prediction (CP) example: {*Amaranthus palmeri* (56%), *Amaranthus spinosus* (44%)} (right)

3.3 Performance Challenges

To further evaluate the model in real-world scenarios, the model was used to test the challenges of model performance due to intra-species dissimilarity and inter-species similarity. The quantitative results are shown in Table 4, and the differences in developmental stages and look-alike species are shown in Figures 9 and Figure 8. The results in intra-species dissimilarity showed that the difficulty in identifying early-stage plants and the model’s accuracy improves significantly through the developmental stages. The model struggles most with identifying look-alike species, particularly grass species.

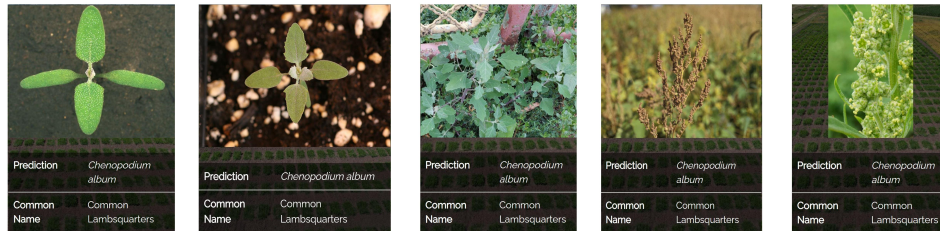
Table 4: Results of model performance for weed identification challenges. The model was tested for the challenges of difference in life stages (intra-species dissimilarity)* and look-alike species(inter-specific similarity)*. Quantitative results in terms of the Accuracy, Macro Precision, Macro Recall, and Macro F1 for model performance

Challenges	Class	Number of testing images	Accuracy	Macro Precision	Macro Recall	Macro F1
Early plant stage	84	151	65.8%	67.0%	61.7%	61.5%
Vegetative stage	84	190	80.2%	86.5%	79.8%	80.8%
Reproductive stage	84	271	85.7%	93.3%	87.0%	89.1%
Life stage*	84	612	79.2%	93.1%	79.6%	83.7%
Amaranthus	8	50	50.0%	57.4%	51.8%	47.7%
Apiaceae	11	61	77.1%	97.4%	77.4%	84.9%
Grass	5	31	45.2%	59.0%	44.0%	50.0%
Look-alike*	24	142	60.6%	76.0%	62.0%	65.3%

3.3.1 Intraspecific dissimilarity

The model’s performance on the weed identification dataset achieved an overall accuracy of 79.2% in the life stage dataset (Table 4: Life stage). When comparing the quantitative results of different development stages, the plant’s early stage has consistently lower accuracy, precision, recall, and F1 than the vegetative and reproductive stages (Table 4). Of 151 images in 84 species, the early stage has 99 misidentified images among 37 species, the vegetative stage has 38 among 22, and the reproductive stage has 37 among 22. The results show that the model performed better in the later growth stages. As illustrated in the intra-species example (Figure 8), early-stage plants have not yet developed most of the phenological traits, displaying only cotyledons and a few true leaves. In contrast, plants in the vegetative stage exhibit fully developed leaves and stems, while those in the reproductive stage show distinct reproductive features, such as flowers and fruits, leading to more accurate identifications. These findings suggest that certain plant families share similar morphological characteristics, especially in the early stages of growth, which challenges the model to distinguish between them. Of the 84 species evaluated, 37 were misidentified in the early growth stage. Grass species were particularly prevalent among misidentifications, with 13 species incorrectly classified, followed by five species of the Aster family. The early stage grass species posed the most significant challenge, as they often lack distinctive morphological characteristics, making it more difficult for the model to differentiate them accurately.

Common lambsquarters (*Chenopodium album*)



Horseweed (*Erigeron canadensis*)

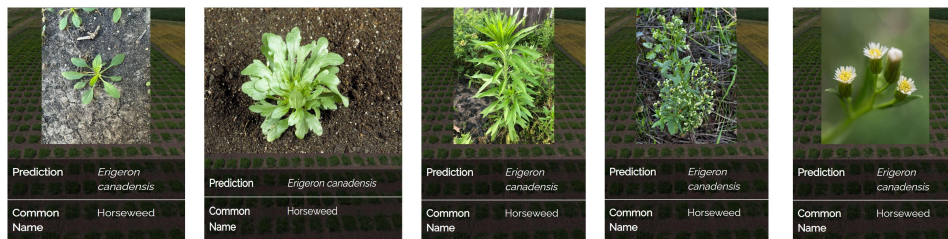


Figure 8: Examples of WeedNet identified intra-species dissimilar weeds through developmental stages. The model accurately identified common lambsquarters (top row) and horseweed (bottom row)

3.3.2 Inter-specific similarity

The model accuracy for the inter-species similarity or look-alike species challenge decreased to 60.6% (Table 4: Look-alike). Comparing the accuracy, Macro precision, Macro recall, and Macro F1 score between overall look-alike and life stage classes indicates that the look-alike challenge is more difficult to distinguish. In addition, the results showed that the model performance varied among different species families (Table 4). The results indicate that the Apiaceae family outperformed both the Amaranthaceae family and the Poaceae family in terms of accuracy, macro precision, macro recall, and macro F1 score (Table 4). The model can reach a relatively high accuracy in them, even if the images focus only on the inflorescence features (Figure 9: Apiaceae). Additionally, 97.4% Macro Precision means that the test species list is a comprehensive data set that covers most look-alike species that develop finely divided leaves and umbrella-like flowers. The MacroPrecision in the amaranth and grass dataset is 57-59%. This indicates that there are other look-alike species not selected among these eight amaranth species and five grass species in the global dataset. This is because many grass species in addition to foxtails in the global dataset and amaranth species have a leaf morphology similar to other broadleaf species in other families. These results further support the conclusion that the phenological similarity between look-alike species poses a major challenge to the model classification performance.

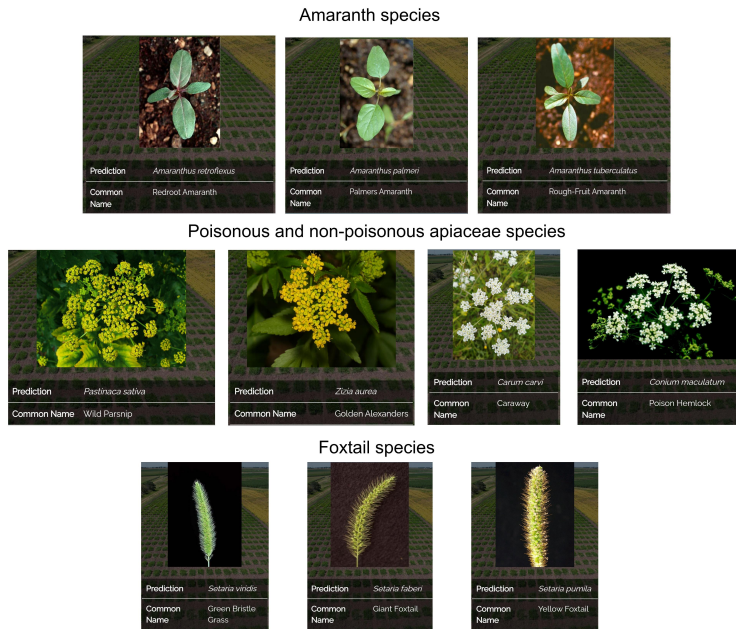


Figure 9: Examples of WeedNet identified inter-species similar weeds in a) Amaranth family b) Apiaceae family c) Grass family

The results in both the life stage and look-alike species datasets show that the grass family is the most difficult family to identify before the spike heading (Table 4). Using knowledge of weed identification, grass species have distinguishable characteristics in the auricle and ligule, and a model can

100% accuracy, and all invasive species had a test accuracy of at least 85%. These results highlight the robustness of the model in identifying invasive species across multiple plant families and environments (Figure 11).

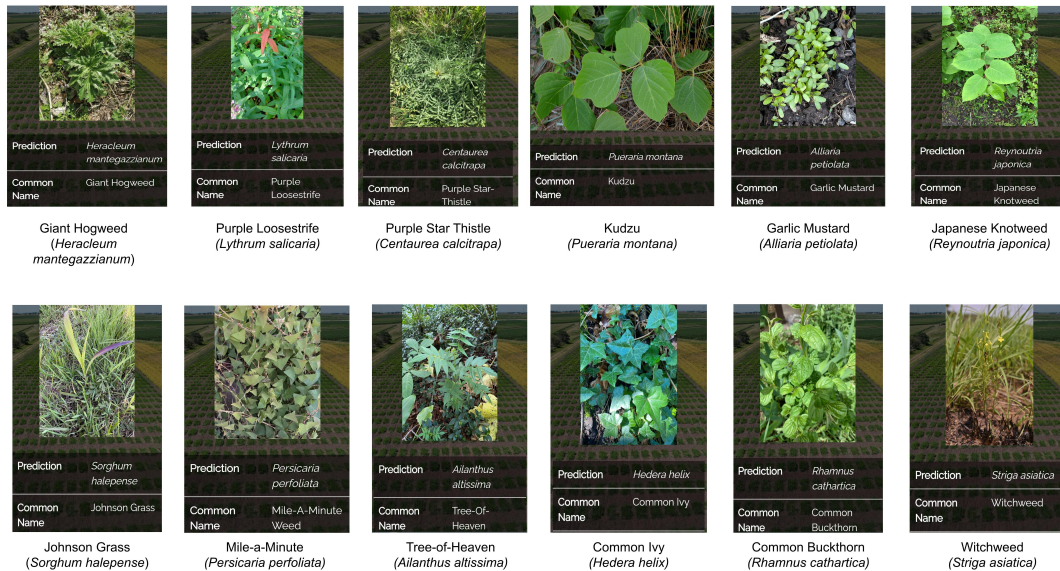


Figure 11: Examples of WeedNet can accurately classify invasive weed species (listed by NISIC, USDA).

3.4 Deployment Challenges

3.4.1 Weed Identification on Robotic Platforms

The WeedNet model was evaluated in two different settings: (i) the targeted identification of 15 specific weed species throughout the evaluation period and (ii) an untargeted visual survey assessing the presence of various weeds in the field (Figure 12). When WeedNet was run on images taken from UAVs and ground-based robots, it accurately identified weeds throughout the season. For both imaging platforms, UAV and ground robot, the WeedNet model demonstrates strong identification performance, showing its ability to monitor consistently across different growth stages. The predictions based on UAVs remained highly comparable to those of the ground robot, reinforcing UAV images' viability for identifying weeds.

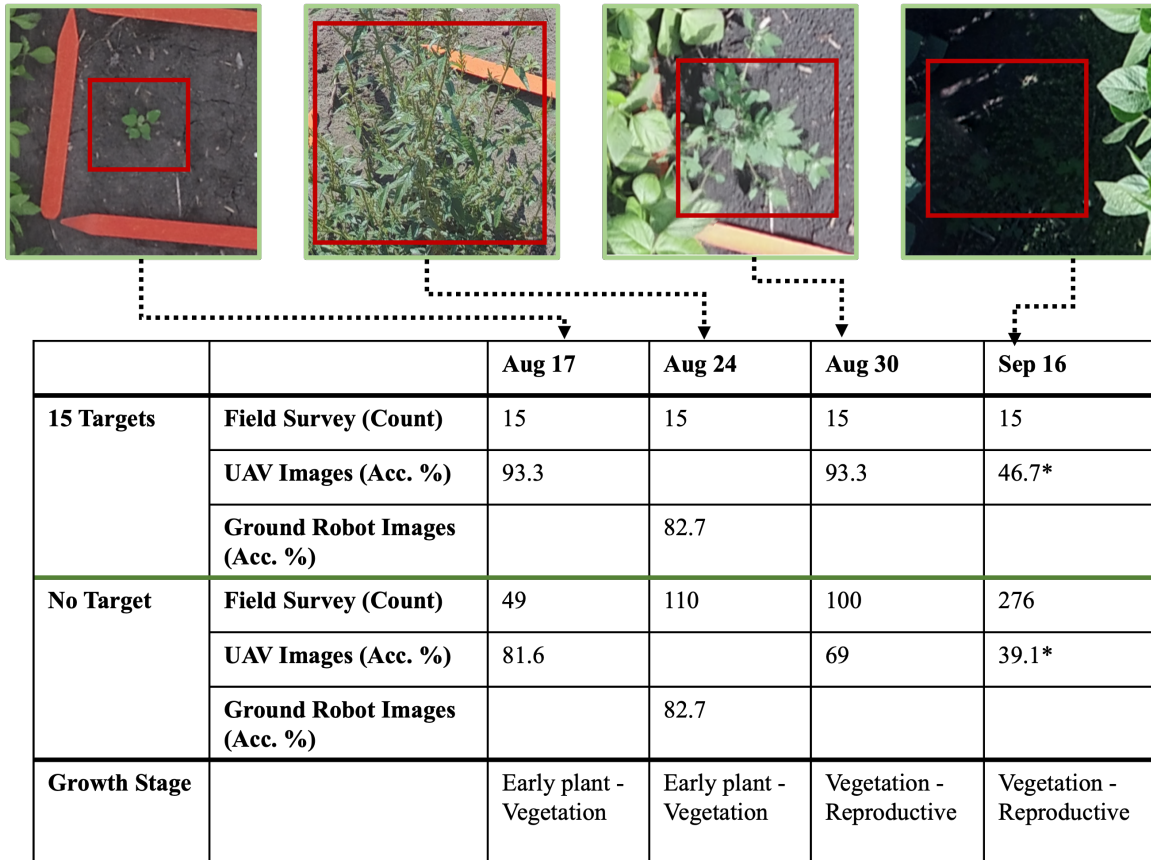


Figure 12: Field evaluation of the WeedNet model using UAV and ground rover data. The model was tested across multiple days (Aug 17, Aug 24, Aug 30, and Sep 16) in the year 2024 under two settings: (i) identification of 15 targeted weed species throughout the evaluation period and (ii) an untargeted visual survey of weeds present in the field. Sample images of randomly observed weeds are shown for each evaluation day. The box within the images highlights the weed in focus. "Amiga" refers to the Farm-ng Amiga ground-based robot. * indicates that weeds were obscured due to overlapping canopy.

In an untargeted setting, randomly sampled images of weeds in the field were analyzed on multiple dates. The accuracy of the model decreased with time and the weed infestation was more severe (Figure 12). Challenges such as increased canopy coverage affected identification accuracy as the season progressed, particularly last time point (Figure 12: 16 September). The overlapping vegetation in the later stages images led to a significant presence of other plant species and overlapping, which may have contributed to identification errors. In addition, canopy shadows and dense vegetation further complicate identification. These observations provide a warning for practitioners to make decisions about when to deploy these robotic platforms for imaging and WeedNet usage. Despite these challenges, the UAV-based model remained an effective tool for large-scale weed surveillance of early-season weeds, which is also the optimal timing of weed control. Moreover, to achieve high crop yield, weed management is necessary when weeds are in early development and before crop canopy closure, and aerial imagery is most useful in these early stages of crop and weed growth since

imaging after canopy closure or weed maturity is of little value [124].

4 Discussion

Data Challenges. This study represents a pioneering effort to use biodiversity science resources to advance AI models for weed classification. The manual annotation process is one of the most labor intensive and time-consuming processes in AI model development [125]. Using publicly available datasets online can significantly reduce the effort and time required to build a training dataset from scratch for AI model development. The extensive collection of images and metadata collected, particularly from the iNaturalist dataset, marks a significant milestone for WeedNet. With more than 14 million images covering 1,593 weed species, this dataset provides unparalleled training data. Most species benefit from more than 500 verified training images, contributed by observers who captured various plant phenotypes, colors, viewpoints, backgrounds, light conditions, and growth stages. This diversity enriches WeedNet’s training capacity and enhances its overall performance. This comprehensive approach contrasts with previous studies, which have often focused on only economically significant or regionally dominant weed species [51, 123, 126, 127]. These models, while effective within their limited scope, lack greater applicability. In contrast, WeedNet is designed for deployment across diverse regions and cropping systems due to its global scale and species diversity.

Furthermore, some studies have developed weed classification models that distinguish mainly between crops and weeds [128–130]. These models typically overlook species-level weed identification, which limits their applicability in precision weed management, where species-specific herbicide recommendations are critical, especially for differentiating between herbicide-resistant and susceptible weed populations. WeedNet includes a diverse range of globally relevant weed species, encompassing invasive, noxious, poisonous, and conserved categories. Furthermore, WeedNet uses scientific and common names for each species, supporting consistent taxonomy and improving the reliability of species-level identification across diverse geographic and agronomic contexts.

Model challenges. The results of the study demonstrate that self-supervised learning and fine-tuning strategies can effectively leverage citizen science data sets to improve the training of the WeedNet model and accurately identify a wide range of weed species. Local models can improve the prediction accuracy for low-performing species by employing a global-to-local fine-tuning strategy. Furthermore, additional fine-tuning with expert-verified datasets leads to a refined Iowa model that outperforms the original version, highlighting the critical importance of both data quality and quantity in model training. These findings underscore the value of incorporating expert-curated data sets and targeted fine-tuning methods to optimize model performance. In weed detection and classification, fine-tuning pre-trained models on any plant data set has enhanced the accuracy of supervised learning algorithms [131].

WeedNet and the fine-tuning approach lead the refined Iowa model to achieve great accuracy across all expert-verified datasets with a small number of training images (see Table 3). This improvement may result from WeedNet serving as a foundational model that already captures most plant characteristics using the existing 1,593-species database, compared to using a generic image database, such as ImageNet, Objects365, or MS COCO, as a pre-trained model [125, 132–134].

The comparison between models demonstrated that the global-to-local strategy could improve the accuracy and adaptability of the model (see Table 1). Fine-tuning the WeedNet model with a local weed species collection can reduce the computational power and image collection resources typically required to develop an accurate local weed classifier.

One notable limitation of WeedNet is the class imbalance within the dataset. Rare weed species often have significantly fewer images than common or invasive species. Our results show that minority species are frequently misclassified as closely related species from the same family, likely due to shared phenological features and a substantially larger number of training images for the latter. This imbalance can lead to overfitting the model in underrepresented classes and introduces bias favoring dominant classes during training [51, 135, 136]. In other domains, class-imbalance learning approaches such as advanced multiclass algorithms [137], transfer learning with resampling [138], or reweighting techniques [139] have been proposed to address this challenge. However, these methods in weed identification require collaboration with weed scientists to define a minority class since species with few images but distinct features can still achieve high classification accuracy. Encouraging farmers, researchers, and agricultural extension workers to contribute labeled images can improve the model’s performance and create a more comprehensive database. WeedNet can overcome inconsistencies in crowd-sourced datasets by integrating expert data with crowd-sourced contributions.

As ensuring the reliability and trustworthiness of WeedNet is critical for its practical applications, we incorporate uncertainty quantification and out-of-distribution detection mechanisms. These features help identify cases where the model lacks confidence, prompting users to seek expert verification [31, 110]. By incorporating confidence scores and providing visual indicators of uncertainty, users can make more informed decisions and mitigate the risks associated with misidentification. These features can also help identify new invasive species in a region when the model consistently reports that the captured weeds are out of distribution, and can help farmers investigate further to identify the invasive species correctly.

Performance challenges. The results of the study tested intra-species dissimilarity, differences in developmental stages and challenges, indicating that the differentiation of plant characteristics drives the model accuracy (see Section 3.3.1). The early plant stage and grass species classes have fewer characteristic features, resulting in lower accuracy and more misidentification than other testing categories. Previous studies also report most misidentification due to similar morphological characteristics, especially during the early stage, where they can only be discriminated against by their texture and color [140, 141].

Furthermore, our results demonstrated that the inter-species similarity significantly decreased the accuracy of the model (Sections 3.2.1 and 3.3.2). Few studies have highlighted the challenge of look-alike species in weed classification, a persistent problem in real-world scenarios. This study demonstrates that look-alike species are one of the main challenges influencing the global-scale weed classification model.

Traditionally, weed identification has relied on farmer or weed specialist observations of a limited number of well-known species, using phenological cues to infer which species are prone to misidentification. This approach can delay the detection of newly emerging or look-alike invasive species.

WeedNet, which includes the most widely known invasive weeds and their classification accuracy, offers a novel way to identify species that are often confused with others. For example, the northern dock is mostly misidentified as a curled dock (see Supplementary Figure S5). It would not be misidentified as a green foxtail, which means species in the Dock family have similar leaf morphology, and these two docks are nearly identical. The identification output of each species tells which species are most commonly misidentified and which species they are confused with, which can further expand to a comprehensive list of look-alike species. This insight can guide the collection of additional images for look-alike species in future studies and help weed scientists pinpoint key distinguishing features for a more accurate identification [142]. The image tests focusing on the grass collars provide information on the importance of identifying and capturing the distinct morphological characteristics of species that are difficult to classify for the end users of the model (Figure 10).

Future research can also explore solutions from other fields facing similar challenges of inter-class similarity and intraclass dissimilarity. For example, aerial scene classification has addressed such issues using Euclidean distances between class feature statistics [136] while embedding learning approaches in face recognition have leveraged softmax dissection techniques [143] to enhance discriminative learning.

Operational/Deployment challenges. The model tested on the images from the robotic platform achieved over 80% accuracy in the early and vegetative stages of the plants for targeted ($n = 15$) and untargeted weed surveys ($n=159$) (Figure 12: Aug17 and Aug24). The increased misidentification was mainly caused by the difficulty of targeting a single plant. These results demonstrated that citizen-sourced images capture weed plants under diverse conditions and that the deep learning model can effectively extract the distinguishing features and perform well on varying platforms.

When comparing manually captured images with those from the robotic platform, the primary difference lies in image resolution and the amount of plant detail captured. Previous studies have shown that image resolution drives the accuracy of individual weed plant discrimination [144, 145]. In particular, the UAV images in this study achieved resolutions of 0.1 to 0.12 cm/pixel, significantly contributing to the model’s effectiveness by preserving fine morphological traits. Meanwhile, a subset of citizen images focused only on specific plant characteristics (e.g., leaves, flowers, or stems), whereas the robotic platform typically captured the entire plant. These differences in citizen datasets and robotic applications highlight the importance of comprehensive plant characteristic coverage and high-resolution image data when training and deploying models for weed discrimination across imaging platforms.

For future applications, WeedNet has the potential to be extended for multi-object classification and object detection in complex field settings. High weed infestations often result in overlapping plants, making it difficult to distinguish between species in a single image. Furthermore, variations in lighting and shading in different parts of the image can pose additional challenges [54]. To address this, the images used in this study could serve as pre-training data to transition WeedNet from an image classification model to an object detection model [125, 146]. Incorporating WeedNet into autonomous platforms such as sprayer drones and precision sprayers would enable real-time species-level weed detection, improving control accuracy, protecting crop yield, reducing input costs and

potential herbicide resistance.

WeedNet can also expand beyond identification to include segmentation and quantification of weed density estimation. Using the trained classification encoder for a segmentation model and explainable AI, images can be segmented to identify the spatial distribution of weeds without significant annotation cost [22, 147]. Farmers can gain insight into weed infestation patterns and plan targeted interventions. Furthermore, density estimation can help quantify the coverage of weeds in fields, providing data-driven recommendations for site-specific weed control. These advancements will enhance the utility of the model, making it an indispensable tool for precision agriculture and large-scale weed management strategies.

Furthermore, WeedNet has practical implications beyond field identification, particularly at critical checkpoints such as US ports of entry, where invasive weed species are frequently intercepted as disseminules, including seeds, fruits, and other plant parts. These propagules often contaminate commercial seed stocks, spices, shipping containers, and baggage. Currently, quarantine officials rely on tools such as the Federal Noxious Weed Disseminules of the United States (FNWD) and visual inspections to detect these threats [148]. The prominent species of concern include giant hogweed, Johnsongrass, Japanese knotweed, and witchweed. The Animal and Plant Health Inspection Service (APHIS), in collaboration with Customs and Border Protection (CBP), inspects incoming shipments and determines appropriate mitigation actions. With its high accuracy and adaptability, the Global WeedID model can be fine-tuned for disseminule-level identification and integrated into port-of-entry workflows. It has the potential to serve as a first line of defense by enabling rapid AI-assisted screening, ultimately supporting expert verification and timely mitigation decisions to prevent the spread of invasive species.

5 Conclusion

The study successfully developed a global scale weed identification model, WeedNet, using a citizen-sourced image repository (iNaturalist) that includes over 14 million images representing 1,593 weed species, encompassing diverse categories such as invasive, poisonous, noxious, and conserved plants. A two-stage training strategy was employed, combining self-supervised learning and fine-tuning with advanced architectures, including Masked Autoencoders (MAE), Vision Transformers, Out-of-Distribution (OOD) detection, and Conformal Prediction (CP) to improve model accuracy, robustness, and trustworthiness in the face of imbalanced datasets. WeedNet achieved outstanding performance, with 91.2% accuracy across all 1,593 species, 97.4% accuracy in 84 Midwest US weed species and 98% accuracy using expert-verified data added for species with conformal prediction. The model was further evaluated for performance under real-world challenges such as intra-species dissimilarity, inter-species similarity, and agriculturally and ecologically relevant invasive weed species, demonstrating that distinguishing morphological traits strongly correlates with accurate classification. Furthermore, the successful prediction of captured images from UAV and robotic platforms confirms the model’s adaptability to varying resolutions, lighting conditions, and overlapping plant instances, highlighting its potential for future real-time weed identification. Integrating WeedNet into PestIDBot establishes its role as a powerful and intelligent decision support tool for farmers

and researchers in modern agriculture.

Funding

This work was supported by the AI Institute for Resilient Agriculture (USDA-NIFA #2021-67021-35329), COALESCE: COntext Aware LEarning for Sustainable CybEr-Agricultural Systems (NSF CPS Frontier #1954556), and USDA CRIS Project IOW04714. The R.F. Baker Center for Plant Breeding, ISU.

Author Contributions

AS and SS designed the project; YS, VNB, ZKD, TTA, MAA, and AR acquired the data; TTA, MS, MAA created new software and/or performed analysis; TTA, MS, YS, AR, VNB, AS, and SS interpreted data; YS, TTA, VNB, MAA, AR, AS, and SS created the first draft; all authors edited, reviewed, and approved the final draft.

Conflicts of Interest

The authors declare that there are no competing interests associated with this work.

Data Availability

We acknowledge iNaturalist as the data source and respect its copyright ownership. Our contribution lies in developing an intuitive pipeline that streamlines data extraction and improves usability for research. The code for replicating our weed identification model is available here: <https://github.com/ttayanlade/WeedsRepo.git>.

Supplementary Materials

S1 Overview of Various Weed Datasets

Table S1: Overview of various weed datasets with details on the number of images, classes, imaging platform, and recognition tasks. MFWD = Moving Fields Weed Dataset. C = Classification, D = Detection, T = Tracking, S = Segmentation

Dataset	Image No.	Class No.	Imaging Platform	Recognition Task
MFWD [149]	94,321	28	Digital Camera	C,D,T,S
CottonWeedDet12 [123]	5,648	12	Digital Cameras	D
CropAndWeed [150]	8,034	74	Digital Cameras	D, S
Weed25 [151]	14,035	25	Digital Camera	D
DeepWeeds [54]	17,509	8	Ground-Based Robot	C
WeedinSoybean [152]	15,336	3	UAV	D



Figure S1: Examples of invasive plant species recorded in the iNaturalist dataset. These invasive plant species are listed by the National Invasive Species Information Center (NISIC), USDA. iNaturalist provides substantial image records of such invasive species, which support efforts in biodiversity monitoring, early detection, and improved management of biological invasions.

S2 List of Weeds

The dataset of 1593 species, all from the Plantae Kingdom and includes eight divisions, seven classes, eighty-one orders, and over a hundred families. The details of the taxonomy for each species are attached in the list of weeds.

S3 Data Preparation

For pretraining, we organize our datasets into varying sizes: 66k, 660k, 2M, and 6M, while for finetuning we used the all of the 14M images, from which we utilized 20 images for training and test sets. Our data processing pipeline involved resizing them to a format of 224x224x3 (height, width, channels) and normalizing their values. To improve our model’s generalizability and robustness, we employed various augmentation techniques to artificially expand the dataset during training. This included geometric and color-space transformations such as flipping, cropping to allow the model perform well under multiple camera positions, and adjustments to brightness and contrast to improve the model’s performance during various times of the day. Additionally, during pretraining, we incorporated advanced augmentation strategies like CutMix, and Mixup-Alpha, which have been shown to significantly improve classification performance. However, we observe a negative effect during finetuning, particularly across look alike species.

S4 Model and Hyperparameters

We utilized a Vision Transformer (ViT) architecture with patch size 14 by 14 and masking as the self-supervised learning (SSL) strategy for pertaining the encoder backbone. The pretrained encoder backbone was subsequently finetuned with a fully connected layer for classification. Both pretraining and fine-tuning were conducted in an end-to-end manner to optimize feature learning and representation. The model was trained for 10 epochs using a batch size of 16 and a base learning rate of $5e-4$. We employed a layer-wise learning rate decay of 0.75 and a weight decay of 0.02 to regulate optimization. Additionally, dropout techniques such as drop path (0.1), stochastic depth regularization, and augmentation strategies, including mixup and cutmix were integrated to improve generalization. Pretraining and finetuning were completed on an A100 GPU cluster, utilizing 8 GPUs and 16 CPUs per task. Each epoch required an average training time of 8 hours.

S5 Zero Shot Evaluation

In the zero-shot evaluation, accuracy was reported on the overlap between our classification model and various benchmark datasets as some classes were present, while others were absent. For CottonWeedDet12, 11 out of 12 classes were common, with the exception of Cutleaf Groundcherry (*Physalis angulata*). In DeepWeeds, 5 classes were common, while Chinee apple (*Ziziphus mauritiana*), Parkinsonia (*Parkinsonia aculeata*), and Siam weed (*Chromolaena odorata*) were not included. For WeedsAI, 15 classes overlapped with our classification list, including *Amaranthus tu-*

berculatus, *Amaranthus palmeri*, *Amaranthus retroflexus*, *Ambrosia artemisiifolia*, *Bassia scoparia*, *Chenopodium album*, *Cryptostegia grandiflora*, *Erigeron canadensis*, *Lantana camara*, *Taraxacum officinale*, *Parthenium hysterophorus*, *Raphanus raphanistrum*, *Vachellia nilotica*, *Xanthium strumarium*, and *Zea mays*.

S6 Comparison of Top-1 and Top-5 accuracy for classifier with different architectures.

Table S2: Top-1 and Top-5 Performance comparison of classifier with different architectures. For the SWAV model, we initialize pretraining using InsectNet weights [31] (a model pretrained and finetuned on insect datasets).

Architecture	Top-1 Accuracy	Top-5 Accuracy
SWAV - RegNetY32	86.67%	95.88%
MAE - Base	86.90%	96.11%

S7 Comparison of Top-1 and Top-5 accuracy for MAE models with different parameter sizes.

Table S3: Comparison of Top-1 and Top-5 accuracy for MAE models with different parameter sizes.

Number of Parameters	Top-1 Accuracy	Top-5 Accuracy
86M	86.90%	96.11%
304M	88.53%	96.84%
633M	89.32%	97.77%

S8 Performance of classifier with varying pre-training dataset sizes.

Table S4: Performance of the classifier with varying pre-training dataset sizes.

Dataset Size	Top-1 Accuracy %	Top-5 Accuracy %
66k	86.21	95.52
660k	86.25	95.84
2M	86.78	96.05
6M	87.95	96.60

S9 PestIDBot



Figure S2: Example of PestIDBot gives the identification and comprehensive information for the species

S10 PestIDBot

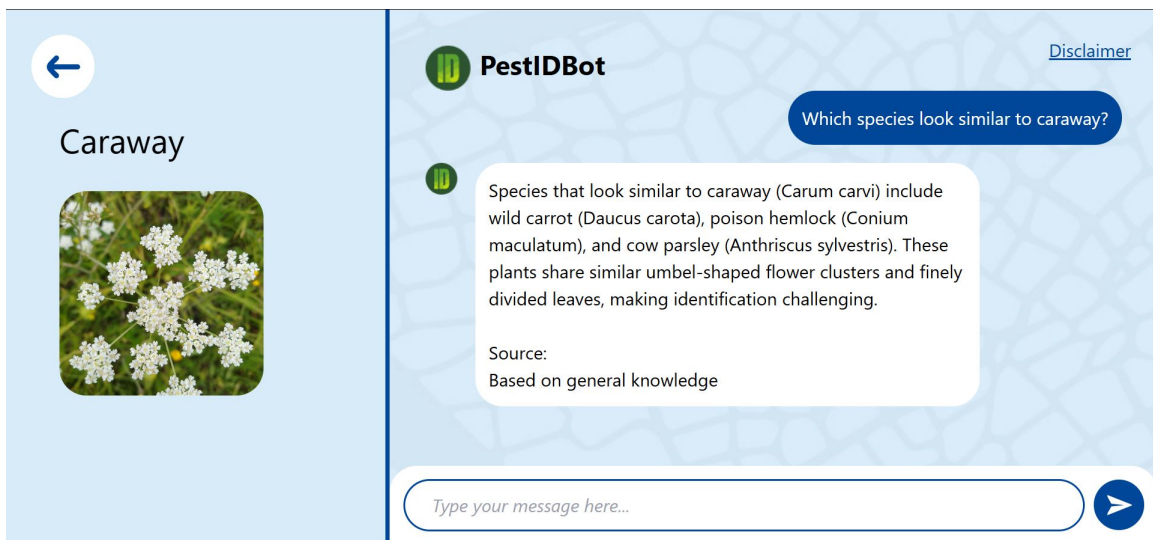


Figure S3: Example of PestIDBot answering the user's question relevant to the identified species

S11 Look-alike species list

Table S5: List of look-alike species to evaluate inter-species similarity

Number of species	Apiales species	Amaranth species	Grass species
1	<i>Achillea millefolium</i>	<i>Amaranthus blitum</i>	<i>Digitaria sanguinalis</i>
2	<i>Aegopodium podagraria</i>	<i>Amaranthus hybridus</i>	<i>Phleum pratense</i>
3	<i>Aethusa cynapium</i>	<i>Amaranthus palmeri</i>	<i>Setaria faberi</i>
4	<i>Cicuta maculata</i>	<i>Amaranthus powellii</i>	<i>Setaria pumila</i>
5	<i>Conium maculatum</i>	<i>Amaranthus retroflexus</i>	<i>Setaria viridis</i>
6	<i>Conopodium majus</i>	<i>Amaranthus spinosus</i>	
7	<i>Daucus carota</i>	<i>Amaranthus tuberculatus</i>	
8	<i>Heracleum mantegazzianum</i>	<i>Amaranthus viridis</i>	
9	<i>Heracleum maximum</i>		
10	<i>Pastinaca sativa</i>		
11	<i>Foeniculum vulgare</i>		

S11.1 Results for low accuracy species

Table S6: List of species with less than 20% accuracy and their identification results for the first testing image. Most misidentifications are to species from the same family having a significantly greater number of training images.

Class	Accuracy (%)	Training Images Count (TIC)	Identification	Acc. (%)	TIC
<i>Avena sterilis</i>	0	297	<i>Avena fatua</i>	90	5001
<i>Chenopodium berlandieri</i>	0	183	<i>Chenopodium album</i>	100	30178
<i>Hedera hibernica</i>	0	588	<i>Hedera helix</i>	100	54057
<i>Pilosella floribunda</i>	0	198	<i>Pilosella caespitosa</i>	90	2950
<i>Tamarix chinensis</i>	0	346	<i>Tamarix ramosissima</i>	100	5593
<i>Tamarix gallica</i>	0	450	<i>Tamarix ramosissima</i>	100	5593
<i>Thunbergia laurifolia</i>	0	208	<i>Thunbergia grandiflora</i>	100	1888
<i>Hedera canariensis</i>	5	893	<i>Hedera helix</i>	100	54057
<i>Rumex longifolius</i>	5	783	<i>Rumex crispus</i>	100	32739
<i>Alopecurus arundinaceus</i>	10	462	<i>Avena fatua</i>	90	5001
<i>Acaena pallida</i>	15	284	<i>Acaena novae-zelandiae</i>	100	3900
<i>Catalpa bignonioides</i>	15	1291	<i>Catalpa speciosa</i>	95	6530
<i>Eucalyptus saligna</i>	15	193	<i>Eucalyptus tereticornis</i>	85	1869
<i>Malus prunifolia</i>	15	200	<i>Malus baccata</i>	80	3699
<i>Malus sylvestris</i>	15	1512	<i>Rhamnus cathartica</i>	100	31215
<i>Wisteria floribunda</i>	15	462	<i>Wisteria sinensis</i>	100	2097

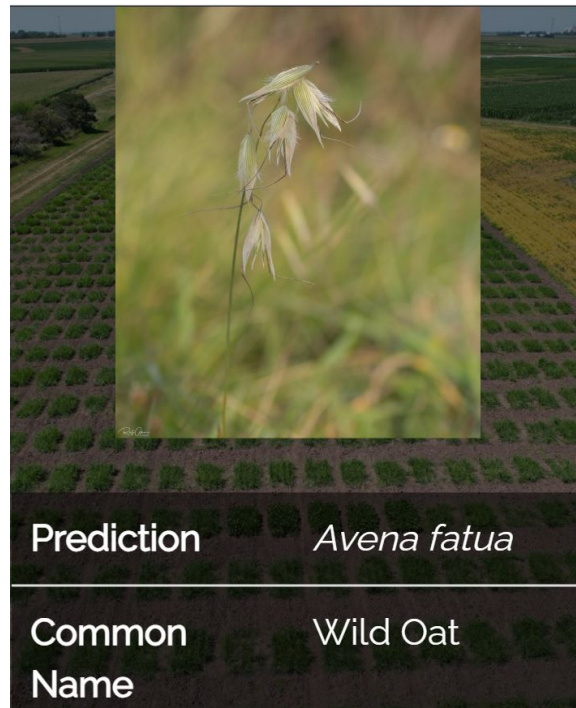


Figure S4: An example of Animated Oat (*Avena sterilis*) misidentified as Wild Oat (*Avena fatua*)

Table S7: Among the 20 testing images of *Avena sterilis*, the majority of misclassifications were identified as *Avena fatua*. Notably, *Avena fatua* has significantly more training images compared to other species within the same family, suggesting a potential bias toward more frequently represented species in the training dataset.

Class	All 20 Testing Images Results
<i>Avena sterilis</i>	<i>Avena fatua</i> <i>Avena fatua</i> <i>Avena fatua</i> <i>Avena barbata</i> <i>Avena barbata</i> <i>Avena fatua</i> <i>Avena fatua</i> <i>Avena fatua</i> <i>Avena fatua</i> <i>Avena barbata</i> <i>Avena barbata</i> <i>Avena fatua</i> <i>Avena barbata</i> <i>Avena fatua</i> <i>Lapsana communis</i> <i>Avena fatua</i> <i>Avena fatua</i> <i>Ranunculus bulbosus</i> <i>Avena fatua</i>

Class	Accuracy (%)	Training Images Count
<i>Avena sterilis</i>	0	297
<i>Avena barbata</i>	65	1923
<i>Avena sativa</i>	65	1251
<i>Avena fatua</i>	90	5001
<i>Lapsana communis</i>	100	29768

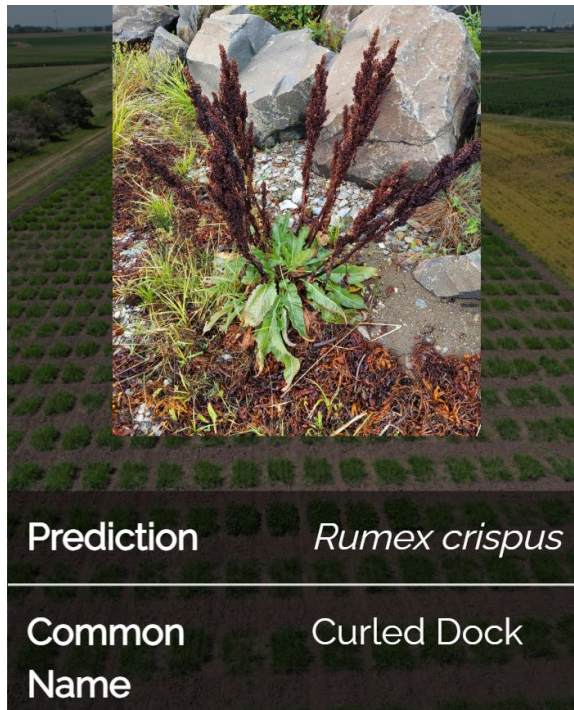


Figure S5: An example of northern dock (*Rumex longifolius*) misidentified as curled cock (*Rumex crispus*)

Table S8: Among the 20 testing images of *Rumex longifolius*, the majority of misclassifications were identified as *Rumex crispus*. Notably, *Rumex crispus* has significantly more training images compared to other species within the same family, suggesting a potential bias toward more frequently represented species in the training dataset.

Class	All 20 Testing Images Results	
<i>Rumex longifolius</i>	<i>Rumex crispus</i> <i>Rumex acetosa</i> <i>Rumex obtusifolius</i> <i>Rumex crispus</i> <i>Rumex acetosa</i> <i>Rumex crispus</i> <i>Rumex crispus</i> <i>Rumex crispus</i> <i>Rumex crispus</i> <i>Rumex crispus</i> <i>Rumex crispus</i> <i>Rumex crispus</i> <i>Rumex crispus</i> <i>Rumex crispus</i> <i>Rumex crispus</i> <i>Verbesina encelioides</i> <i>Rumex longifolius</i> <i>Rumex pseudonatronatus</i> <i>Rumex pseudonatronatus</i> <i>Rumex crispus</i>	
Class	Accuracy (%)	Training Images Count
<i>Rumex crispus</i>	100	32739
<i>Rumex obtusifolius</i>	95	24950
<i>Rumex acetosella</i>	95	22909
<i>Rumex acetosa</i>	80	7542
<i>Rumex maritimus</i>	95	2165
<i>Rumex pseudonatronatus</i>	55	1877
<i>Rumex spinosus</i>	100	1018
<i>Rumex stenophyllus</i>	45	662
<i>Rumex altissimus</i>	80	478
<i>Rumex hypogaeus</i>	65	218
<i>Rumex longifolius</i>	5	783

References

1. Aldrich RJ and Kremer RJ. Principles in weed management. Ed. 2. Ames, IA: Iowa State University Press, 1997:455.
2. Soltani N, Dille JA, Burke IC, et al. Potential corn yield losses from weeds in North America. *Weed Technology* 2016;30:979–84.
3. Flessner ML, Burke IC, Dille JA, et al. Potential wheat yield loss due to weeds in the United States and Canada. *Weed Technology* 2021;35:916–23.
4. Soltani N, Dille JA, Gulden RH, et al. Potential yield loss in dry bean crops due to weeds in the United States and Canada. *Weed Technology* 2018;32:342–6.
5. Christensen S, Sogaard HT, Kudsk P, et al. Site-specific weed control technologies. *Weed Research* 2009;49:233–41.
6. National Invasive Species Information Center. What are Invasive Species? Accessed: 2025-03-27. 2025. URL: <https://www.invasivespeciesinfo.gov/what-are-invasive-species>.
7. Butler JL and Cogan DR. Leafy spurge effects on patterns of plant species richness. *Journal of range management* 2004;57:305–11.
8. Oliveira MC, Jhala AJ, Bernards ML, Proctor CA, Stepanovic S, and Werle R. Palmer amaranth (*Amaranthus palmeri*) adaptation to US Midwest agroecosystems. *Frontiers in Agronomy* 2022;4:887629.
9. Tataridas A, Jabran K, Kanatas P, Oliveira RS, Freitas H, and Travlos I. Early detection, herbicide resistance screening, and integrated management of invasive plant species: a review. *Pest Management Science* 2022;78:3957–72.
10. Green JM and Owen MD. Herbicide-resistant crops: utilities and limitations for herbicide-resistant weed management. *Journal of agricultural and food chemistry* 2011;59:5819–29.
11. Kniss AR. Genetically engineered herbicide-resistant crops and herbicide-resistant weed evolution in the United States. *Weed Science* 2018;66:260–73.
12. Lillie K, Giacomini D, and Tranel P. Comparing responses of sensitive and resistant populations of Palmer amaranth (*Amaranthus palmeri*) and waterhemp (*Amaranthus tuberculatus* var. *rudis*) to PPO inhibitors. *Weed technology* 2020;34:140–6.
13. Weed Science Society of America. Weed Science Society of America Database. <https://www.weedscience.org/Home.aspx>. Accessed: 2025-02-11.
14. Wang P, Peteinatos G, Efthimiadou A, and Ma W. Weed identification and integrated control. 2023.
15. Roberts J and Florentine S. Advancements and developments in the detection and control of invasive weeds: A global review of the current challenges and future opportunities. *Weed Science* 2024:1–29.
16. Verloove F. Invaders in disguise. Conservation risks derived from misidentification of invasive plants. *Management of Biological invasions* 2010:1–5.

17. Marble SC and Brown SH. Invasive plants with native lookalikes: How mistaken identities can lead to more significant plant invasions and delay management. *HortTechnology* 2021;31:385–94.
18. Chen Y, Wu Z, Zhao B, Fan C, and Shi S. Weed and corn seedling detection in field based on multi feature fusion and support vector machine. *Sensors* 2020;21:212.
19. Fathi Kazerouni M, Mohammed Saeed NT, and Kuhnert KD. Fully-automatic natural plant recognition system using deep neural network for dynamic outdoor environments. *SN Applied Sciences* 2019;1:756.
20. Maxwell BD, Lehnhoff E, and Rew LJ. The rationale for monitoring invasive plant populations as a crucial step for management. *Invasive Plant Science and Management* 2009;2:1–9.
21. Adkins S and Shabbir A. Biology, ecology and management of the invasive parthenium weed (*Parthenium hysterophorus* L.) *Pest management science* 2014;70:1023–9.
22. Adhinata FD, Sumiharto R, et al. A comprehensive survey on weed and crop classification using machine learning and deep learning. *Artificial intelligence in agriculture* 2024.
23. Khaire P, Attar V, and Kalamkar S. A Comprehensive Survey of Weed Detection and Classification Datasets for Precision Agriculture. In: *2023 14th International Conference on Computing Communication and Networking Technologies (ICCCNT)*. IEEE. 2023:1–5.
24. Murad NY, Mahmood T, Forkan ARM, Morshed A, Jayaraman PP, and Siddiqui MS. Weed detection using deep learning: A systematic literature review. *Sensors* 2023;23:3670.
25. Bouguettaya A, Zarzour H, Kechida A, and Taberkit AM. Deep learning techniques to classify agricultural crops through UAV imagery: A review. *Neural computing and applications* 2022;34:9511–36.
26. Upadhyay A, Zhang Y, Koparan C, et al. Advances in ground robotic technologies for site-specific weed management in precision agriculture: A review. *Computers and Electronics in Agriculture* 2024;225:109363.
27. Jafar A, Bibi N, Naqvi RA, Sadeghi-Niaraki A, and Jeong D. Revolutionizing agriculture with artificial intelligence: plant disease detection methods, applications, and their limitations. *Frontiers in Plant Science* 2024;15:1356260.
28. Li L, Zhang S, and Wang B. Plant disease detection and classification by deep learning—a review. *IEEE Access* 2021;9:56683–98.
29. Bhargava A, Shukla A, Goswami OP, Alsharif MH, Uthansakul P, and Uthansakul M. Plant leaf disease detection, classification, and diagnosis using computer vision and artificial intelligence: A review. *IEEE access* 2024;12:37443–69.
30. Toscano-Miranda R, Toro M, Aguilar J, Caro M, Marulanda A, and Trebilcok A. Artificial-intelligence and sensing techniques for the management of insect pests and diseases in cotton: a systematic literature review. *The Journal of Agricultural Science* 2022;160:16–31.
31. Chiranjeevi S, Saadati M, Deng ZK, et al. InsectNet: Real-time identification of insects using an end-to-end machine learning pipeline. *PNAS nexus* 2025;4:pgae575.

32. Partel V, Kakarla SC, and Ampatzidis Y. Development and evaluation of a low-cost and smart technology for precision weed management utilizing artificial intelligence. *Computers and electronics in agriculture* 2019;157:339–50.
33. Murphy KM, Ludwig E, Gutierrez J, and Gehan MA. Deep learning in image-based plant phenotyping. *Annual Review of Plant Biology* 2024;75.
34. Deng B, Lu Y, and Xu J. Weed database development: An updated survey of public weed datasets and cross-season weed detection adaptation. *Ecological Informatics* 2024;81:102546.
35. Li Y, Al-Sarayreh M, Irie K, et al. Identification of weeds based on hyperspectral imaging and machine learning. *Frontiers in Plant Science* 2021;11:611622.
36. Rasmussen J, Azim S, and Nielsen J. Pre-harvest weed mapping of *Cirsium arvense* L. based on free satellite imagery—The importance of weed aggregation and image resolution. *European Journal of Agronomy* 2021;130:126373.
37. Martin FM, Müllerová J, Borgniet L, Dommanget F, Breton V, and Evette A. Using single- and multi-date UAV and satellite imagery to accurately monitor invasive knotweed species. *Remote Sensing* 2018;10:1662.
38. Xu M, Yoon S, Wu C, Baek J, and Park DS. PlantCLEF2023: A Bigger Training Dataset Contributes More than Advanced Pretraining Methods for Plant Identification. In: *CLEF (Working Notes)*. 2023:2168–80.
39. Goëau H, Bonnet P, and Joly A. Overview of PlantCLEF 2023: image-based plant identification at global scale. In: *CLEF 2023 Working Notes-24th Conference and Labs of the Evaluation Forum*. Vol. 3497. 2023:1972–81.
40. Joly A, Picek L, Kahl S, et al. Overview of lifeclef 2024: Challenges on species distribution prediction and identification. In: *International Conference of the Cross-Language Evaluation Forum for European Languages*. Springer. 2024:183–207.
41. Coleman GR, Bender A, Hu K, et al. Weed detection to weed recognition: reviewing 50 years of research to identify constraints and opportunities for large-scale cropping systems. *Weed Technology* 2022;36:741–57.
42. Lu Y and Young S. A survey of public datasets for computer vision tasks in precision agriculture. *Computers and Electronics in Agriculture* 2020;178:105760.
43. Sunil G, Koparan C, Upadhyay A, et al. A novel automated cloud-based image datasets for high throughput phenotyping in weed classification. *Data in Brief* 2024;57:111097.
44. Venkataraju A, Arumugam D, Kiran R, and Peters T. Automated approaches for the early stage distinguishing of Palmer amaranth from waterhemp. *Frontiers in Agronomy* 2024;6:1425425.
45. Fried G, Norton LR, and Reboud X. Environmental and management factors determining weed species composition and diversity in France. *Agriculture, ecosystems & environment* 2008;128:68–76.
46. iNaturalist. Observation: 180115803. Accessed: 2025-05-23. 2023. URL: <https://www.inaturalist.org/observations/180115803>.

47. White E, Soltis PS, Soltis DE, and Guralnick R. Quantifying error in occurrence data: Comparing the data quality of iNaturalist and digitized herbarium specimen data in flowering plant families of the southeastern United States. *Plos one* 2023;18:e0295298.
48. Ahmed F, Al-Mamun HA, Bari AH, Hossain E, and Kwan P. Classification of crops and weeds from digital images: A support vector machine approach. *Crop Protection* 2012;40:98–104.
49. Bakhshipour A and Jafari A. Evaluation of support vector machine and artificial neural networks in weed detection using shape features. *Computers and Electronics in Agriculture* 2018;145:153–60.
50. Yano IH, Alves JR, Santiago WE, and Mederos BJ. Identification of weeds in sugarcane fields through images taken by UAV and Random Forest classifier. *IFAC-PapersOnLine* 2016;49:415–20.
51. Chen D, Lu Y, Li Z, and Young S. Performance evaluation of deep transfer learning on multi-class identification of common weed species in cotton production systems. *Computers and Electronics in Agriculture* 2022;198:107091.
52. Hu K, Coleman G, Zeng S, Wang Z, and Walsh M. Graph weeds net: A graph-based deep learning method for weed recognition. *Computers and electronics in agriculture* 2020;174:105520.
53. Du Y, Zhang G, Tsang D, and Jawed MK. Deep-cnn based robotic multi-class under-canopy weed control in precision farming. In: *2022 International Conference on Robotics and Automation (ICRA)*. IEEE. 2022:2273–9.
54. Olsen A, Konovalov DA, Philippa B, et al. DeepWeeds: A multiclass weed species image dataset for deep learning. *Scientific reports* 2019;9:2058.
55. Khan S, Tufail M, Khan MT, Khan ZA, Iqbal J, and Alam M. A novel semi-supervised framework for UAV based crop/weed classification. *Plos one* 2021;16:e0251008.
56. Nong C, Fan X, and Wang J. Semi-supervised learning for weed and crop segmentation using UAV imagery. *Frontiers in Plant Science* 2022;13:927368.
57. Nam H, Lee H, Park J, Yoon W, and Yoo D. Reducing domain gap by reducing style bias. *Proceedings of the IEEE/CVF Conference on Computer Vision and Pattern Recognition* 2021:8690–9.
58. Vaswani A, Shazeer N, Parmar N, et al. Attention is all you need. *Advances in neural information processing systems* 2017;30.
59. Dong J, Chen S, Miralinaghi M, Chen T, and Labi S. Development and testing of an image transformer for explainable autonomous driving systems. *Journal of Intelligent and Connected Vehicles* 2022;5:235–49.
60. Thai HT, Le KH, and Nguyen NLT. FormerLeaf: An efficient vision transformer for Cassava Leaf Disease detection. *Computers and Electronics in Agriculture* 2023;204:107518.
61. Huang X, Kroening D, Kwiatkowska M, et al. Safety and trustworthiness of deep neural networks: A survey. *arXiv preprint arXiv:1812.08342* 2018:151.

62. Deng A, Li S, Xiong M, Chen Z, and Hooi B. Trust, but verify: Using self-supervised probing to improve trustworthiness. In: *European Conference on Computer Vision*. Springer. 2022:361–77.
63. Nagasubramanian K, Jubery T, Fotouhi Ardakani F, et al. How useful is active learning for image-based plant phenotyping? *The Plant Phenome Journal* 2021;4:e20020.
64. Borgy B, Perronne R, Kohler C, Grison AL, Amiaud B, and Gaba S. Changes in functional diversity and intraspecific trait variability of weeds in response to crop sequences and climate. *Weed Research* 2016;56:102–13.
65. Baker HG. The evolution of weeds. *Annual review of ecology and systematics* 1974:1–24.
66. Goolsby JA, De Barro PJ, Makinson JR, Pemberton RW, Hartley DM, and Frohlich DR. Matching the origin of an invasive weed for selection of a herbivore haplotype for a biological control programme. *Molecular Ecology* 2006;15:287–97.
67. Alvarez-Fernandez R. *Herbicides: Environmental Impact Studies and Management Approaches*. BoD–Books on Demand, 2012.
68. Boisseau RP, Bradler S, and Emlen DJ. Divergence time and environmental similarity predict the strength of morphological convergence in stick and leaf insects. *Proceedings of the National Academy of Sciences* 2025;122:e2319485121.
69. Treher A, Lenny Wilson RN, and Kuehn FB. *Invasive Plants and their Native Look-alikes: An Identification Guide for the Mid-Atlantic*. https://www.nybg.org/files/scientists/rnaczi/Mistaken_Identity_Final.pdf. Accessed: 2024-07-16. 2024.
70. Sun H, Chu S, Jiang L, et al. Integrative analysis of chloroplast genome, chemicals, and illustrations in Bencao literature provides insights into the medicinal value of *Peucedanum huangshanense*. *Frontiers in Plant Science* 2023;14:1179915.
71. University of Maryland Extension. Know Your Foxtail. <https://extension.umd.edu/resource/know-your-foxtails-fs-2023-0658>. Accessed: 2025-02-11. 2023.
72. Eplee RE. Witchweed (*Striga asiatica*): an overview of management strategies in the USA. *Crop Protection* 1992;11:3–7.
73. Harron P, Joshi O, Edgar CB, Paudel S, and Adhikari A. Predicting Kudzu (*Pueraria montana*) spread and its economic impacts in timber industry: A case study from Oklahoma. *PloS one* 2020;15:e0229835.
74. Williams F, Eschen R, Harris A, et al. The economic cost of invasive non-native species on Great Britain. *CABI Proj No VM10066* 2010;199.
75. Werle R, Mobli A, DeWerff RP, and Arneson NJ. Evaluation of foliar-applied post-emergence corn–soybean herbicides on giant ragweed and waterhemp control in Wisconsin. *Agrosystems, Geosciences & Environment* 2023;6:e20338.
76. Urban JM and Leach H. Biology and management of the spotted lanternfly, *Lycorma delicatula* (Hemiptera: Fulgoridae), in the United States. *Annual Review of Entomology* 2023;68:151–67.

77. Heimpel GE, Frelich LE, Landis DA, et al. European buckthorn and Asian soybean aphid as components of an extensive invasional meltdown in North America. *Biological Invasions* 2010;12:2913–31.
78. Boukari W, Wei C, Tang L, et al. Lack of transmission of Sugarcane yellow leaf virus in Florida from Columbus grass and sugarcane to sugarcane with aphids or mites. *PLoS One* 2020;15:e0230066.
79. Rodriguez-Algaba J, Hovmøller MS, Schulz P, et al. Stem rust on barberry species in Europe: Host specificities and genetic diversity. *Frontiers in Genetics* 2022;13:988031.
80. Lahiri S and Reisig DD. Ecology and management of kudzu bug (Hemiptera: Plataspidae) in Southeastern soybeans. *Journal of Integrated Pest Management* 2016;7:14.
81. Paleyes A, Urma RG, and Lawrence ND. Challenges in deploying machine learning: a survey of case studies. *ACM computing surveys* 2022;55:1–29.
82. Sarkar S, Ganapathysubramanian B, Singh A, et al. Cyber-agricultural systems for crop breeding and sustainable production. *Trends in Plant Science* 2024;29:130–49.
83. Program MSUEIP. Plant Identification Apps: Not All Are Created Equal. Accessed: 2025-04-17. 2022. URL: <https://www.montana.edu/extension/invasiveplants/extension/monthly-weed-posts/2022-april-plant-identification-apps.html>.
84. Extension MSU. Plant identification? There’s an app for that – actually several. <https://www.canr.msu.edu/news/plant-identification-theres-an-app-for-that-actually-several>. Accessed: 2025-03-16. 2024.
85. Koh PW, Sagawa S, Marklund H, et al. Wilds: A benchmark of in-the-wild distribution shifts. In: *International conference on machine learning*. PMLR. 2021:5637–64.
86. Dosovitskiy A, Beyer L, Kolesnikov A, Weissenborn D, and Zhai X. Thomas unterthiner mostafa dehghani matthias minderer georg heigold sylvain gelly jakob uszkoreit and neil houlby. An image isworth 16× 16 words: transformers for image recognition atscale. In: *International Conference on Learning Representations*. 2021.
87. Weiss K, Khoshgoftaar TM, and Wang D. A survey of transfer learning. *Journal of Big data* 2016;3:1–40.
88. Sharif Razavian A, Azizpour H, Sullivan J, and Carlsson S. CNN features off-the-shelf: an astounding baseline for recognition. In: *Proceedings of the IEEE conference on computer vision and pattern recognition workshops*. 2014:806–13.
89. iNaturalist. iNaturalist: Observations and User Statistics. Accessed: 2025-03-16. 2025. URL: <https://www.inaturalist.org/stats>.
90. National Invasive Species Information Center. Invasive Species Profiles List. Accessed: 2024-07-16. 2024. URL: <https://www.invasivespeciesinfo.gov/species-profiles-list>.
91. Midwest Invasive Plant Network. Midwest Invasive Plant List. <https://mipn.org/invasive-plant-list/>. Accessed: 2025-02-11. 2023.

92. Invasive Species Web Portal. Invasive and Exotic Weeds. <https://www.invasive.org/species/weeds.cfm>. Accessed: 2025-02-11. 2023.
93. Singh M, Gustafson L, Adcock A, et al. Revisiting weakly supervised pre-training of visual perception models. In: *Proceedings of the IEEE/CVF Conference on Computer Vision and Pattern Recognition*. 2022:804–14.
94. Mahajan D, Girshick R, Ramanathan V, et al. Exploring the limits of weakly supervised pretraining. In: *Proceedings of the European conference on computer vision (ECCV)*. 2018:181–96.
95. Autoencoders SD. Learning useful representations in a deep network with a local denoising criterion, Pascal Vincent, Hugo Larochelle, Isabelle Lajoie, Yoshua Bengio and Pierre-Antoine Manzagol. *J. Mach. Learn. Res.* 11 2010:3371–408.
96. Chen T, Kornblith S, Norouzi M, and Hinton G. A simple framework for contrastive learning of visual representations. In: *International conference on machine learning*. PMLR. 2020:1597–607.
97. Assran M, Duval Q, Misra I, et al. Self-supervised learning from images with a joint-embedding predictive architecture. In: *Proceedings of the IEEE/CVF Conference on Computer Vision and Pattern Recognition*. 2023:15619–29.
98. Zhou J, Wei C, Wang H, et al. ibot: Image bert pre-training with online tokenizer. arXiv preprint arXiv:2111.07832 2021.
99. Dosovitskiy A. An image is worth 16x16 words: Transformers for image recognition at scale. arXiv preprint arXiv:2010.11929 2020.
100. Bao H, Dong L, Piao S, and Wei F. Beit: Bert pre-training of image transformers. arXiv preprint arXiv:2106.08254 2021.
101. He K, Chen X, Xie S, Li Y, Dollár P, and Girshick R. Masked autoencoders are scalable vision learners. In: *Proceedings of the IEEE/CVF conference on computer vision and pattern recognition*. 2022:16000–9.
102. Tong Z, Song Y, Wang J, and Wang L. Videomae: Masked autoencoders are data-efficient learners for self-supervised video pre-training. *Advances in neural information processing systems* 2022;35:10078–93.
103. Girdhar R, El-Nouby A, Singh M, Alwala KV, Joulin A, and Misra I. Omnimae: Single model masked pretraining on images and videos. In: *Proceedings of the IEEE/CVF conference on computer vision and pattern recognition*. 2023:10406–17.
104. Iowa State University Extension and Outreach. Weed Identification Field Guide, 2nd Edition. A reference for identifying weeds in field crops. Iowa State University, 2024. URL: <https://store.extension.iastate.edu/product/Weed-Identification-Field-Guide-2nd-Edition>.
105. Roy AG, Ren J, Azizi S, et al. Does your dermatology classifier know what it doesn't know? detecting the long-tail of unseen conditions. *Medical Image Analysis* 2022;75:102274.

106. Hendrycks D, Mazeika M, and Dietterich T. Deep anomaly detection with outlier exposure. arXiv preprint arXiv:1812.04606 2018.
107. Ren J, Liu PJ, Fertig E, et al. Likelihood ratios for out-of-distribution detection. *Advances in neural information processing systems* 2019;32.
108. Liu W, Wang X, Owens J, and Li Y. Energy-based out-of-distribution detection. *Advances in Neural Information Processing Systems* 2020;33:21464–75.
109. Hendrycks D and Gimpel K. A baseline for detecting misclassified and out-of-distribution examples in neural networks. arXiv preprint arXiv:1610.02136 2016.
110. Saadati M, Balu A, Chiranjeevi S, et al. Out-of-Distribution Detection Algorithms for Robust Insect Classification. *Plant Phenomics* 2024;6:0170.
111. Wang Z, Wang G, Huang B, et al. Masked face recognition dataset and application. arXiv preprint arXiv:2003.09093 2020.
112. Russakovsky O, Deng J, Su H, et al. ImageNet Large Scale Visual Recognition Challenge. *International Journal of Computer Vision (IJCV)* 2015;115:211–52.
113. Angelopoulos AN, Bates S, et al. Conformal prediction: A gentle introduction. *Foundations and Trends® in Machine Learning* 2023;16:494–591.
114. Chiranjeevi S, Sadaati M, Deng ZK, et al. Deep learning powered real-time identification of insects using citizen science data. arXiv preprint arXiv:2306.02507 2023.
115. University of Maryland Extension. Know Your Foxtails. Accessed: 2025-01-24. 2023. URL: <https://extension.umd.edu/resource/know-your-foxtails-fs-2023-0658/>.
116. University of Maryland Extension. Keys to Identifying Palmer Amaranth and Waterhemp. Accessed: 2025-01-24. 2023. URL: <https://extension.umd.edu/resource/keys-identifying-palmer-amaranth-and-waterhemp-fs-2023-0653/>.
117. Sohn SI, Oh YJ, Pandian S, et al. Identification of Amaranthus species using visible-near-infrared (vis-NIR) spectroscopy and machine learning methods. *Remote Sensing* 2021;13:4149.
118. Penn State Extension. Dead Nettle, Henbit, and Ground Ivy: Three Look-Alike Weeds. Accessed: 2025-01-24. URL: <https://extension.psu.edu/dead-nettle-henbit-and-ground-ivy-three-look-alike-weeds>.
119. PestIDBot: An Integrated Solution for End-to-End Agricultural Pest Management. <https://pestid.github.io>. Accessed: 2024-11-16. 2024.
120. Eckert I, Bruneau A, Metsger DA, Joly S, Dickinson T, and Pollock LJ. Herbarium collections remain essential in the age of community science. *Nature Communications* 2024;15:7586.
121. Chiranjeevi S, Saadati M, Deng ZK, et al. InsectNet: Real-time identification of insects using an end-to-end machine learning pipeline. *PNAS Nexus* 2024;4:pgae575.
122. Group PWC and Hub SI. Weed-AI: A Repository of Weed Images in Crops. <https://weed-ai.sydney.edu.au/>. Accessed: 2025-01-20. 2025.

123. Dang F, Chen D, Lu Y, and Li Z. YOLOWeeds: A novel benchmark of YOLO object detectors for multi-class weed detection in cotton production systems. *Computers and Electronics in Agriculture* 2023;205:107655.
124. Torres-Sánchez J, López-Granados F, De Castro AI, and Peña-Barragán JM. Configuration and specifications of an unmanned aerial vehicle (UAV) for early site specific weed management. *PloS one* 2013;8:e58210.
125. Russakovsky O, Deng J, Su H, et al. Imagenet large scale visual recognition challenge. *International journal of computer vision* 2015;115:211–52.
126. Belissent N, Peña JM, Mesías-Ruiz GA, Shawe-Taylor J, and Pérez-Ortiz M. Transfer and zero-shot learning for scalable weed detection and classification in UAV images. *Knowledge-Based Systems* 2024;292:111586.
127. Saini P and Nagesh D. CottonWeeds: Empowering precision weed management through deep learning and comprehensive dataset. *Crop Protection* 2024;181:106675.
128. Moazzam SI, Nawaz T, Qureshi WS, Khan US, and Tiwana MI. A w-shaped convolutional network for robust crop and weed classification in agriculture. *Precision Agriculture* 2023;24:2002–18.
129. Wang A, Xu Y, Wei X, and Cui B. Semantic segmentation of crop and weed using an encoder-decoder network and image enhancement method under uncontrolled outdoor illumination. *Ieee Access* 2020;8:81724–34.
130. Umamaheswari S and Jain AV. Encoder–decoder architecture for crop-weed classification using pixel-wise labelling. In: *2020 International Conference on Artificial Intelligence and Signal Processing (AISP)*. IEEE. 2020:1–6.
131. Hasan AM, Sohel F, Diepeveen D, Laga H, and Jones MG. A survey of deep learning techniques for weed detection from images. *Computers and electronics in agriculture* 2021;184:106067.
132. Jiang P, Ergu D, Liu F, Cai Y, and Ma B. A Review of Yolo algorithm developments. *Procedia computer science* 2022;199:1066–73.
133. Lin TY, Maire M, Belongie S, et al. Microsoft coco: Common objects in context. In: *Computer vision–ECCV 2014: 13th European conference, zurich, Switzerland, September 6-12, 2014, proceedings, part v 13*. Springer. 2014:740–55.
134. Shao S, Li Z, Zhang T, et al. Objects365: A large-scale, high-quality dataset for object detection. In: *Proceedings of the IEEE/CVF international conference on computer vision*. 2019:8430–9.
135. Yang Y and Xu Z. Rethinking the value of labels for improving class-imbalanced learning. *Advances in neural information processing systems* 2020;33:19290–301.
136. Jing C, Huang L, Cai S, et al. Interclass similarity transfer for imbalanced aerial scene classification. *IEEE Geoscience and Remote Sensing Letters* 2023;20:1–5.

137. Bi J and Zhang C. An empirical comparison on state-of-the-art multi-class imbalance learning algorithms and a new diversified ensemble learning scheme. *Knowledge-Based Systems* 2018;158:81–93.
138. Huang C, Li Y, Loy CC, and Tang X. Learning deep representation for imbalanced classification. In: *Proceedings of the IEEE conference on computer vision and pattern recognition*. 2016:5375–84.
139. Shen L, Lin Z, and Huang Q. Relay backpropagation for effective learning of deep convolutional neural networks. In: *Computer Vision–ECCV 2016: 14th European Conference, Amsterdam, The Netherlands, October 11–14, 2016, Proceedings, Part VII 14*. Springer. 2016:467–82.
140. Perez-Ortiz M, Pena JM, Gutierrez PA, Torres-Sanchez J, Hervás-Martínez C, and López-Granados F. Selecting patterns and features for between-and within-crop-row weed mapping using UAV-imagery. *Expert Systems with Applications* 2016;47:85–94.
141. Peteinatos GG, Reichel P, Karouta J, Andújar D, and Gerhards R. Weed identification in maize, sunflower, and potatoes with the aid of convolutional neural networks. *Remote Sensing* 2020;12:4185.
142. Malik OA, Faisal M, and Hussein BR. Ensemble deep learning models for fine-grained plant species identification. In: *2021 IEEE Asia-Pacific Conference on Computer Science and Data Engineering (CSDE)*. IEEE. 2021:1–6.
143. He L, Wang Z, Li Y, and Wang S. Softmax dissection: Towards understanding intra-and inter-class objective for embedding learning. In: *Proceedings of the AAAI conference on artificial intelligence*. Vol. 34. 07. 2020:10957–64.
144. Peña JM, Torres-Sánchez J, Serrano-Pérez A, De Castro AI, and López-Granados F. Quantifying efficacy and limits of unmanned aerial vehicle (UAV) technology for weed seedling detection as affected by sensor resolution. *Sensors* 2015;15:5609–26.
145. Huang Y, Reddy KN, Fletcher RS, and Pennington D. UAV low-altitude remote sensing for precision weed management. *Weed technology* 2018;32:2–6.
146. Zhao Z, Alzubaidi L, Zhang J, Duan Y, and Gu Y. A comparison review of transfer learning and self-supervised learning: Definitions, applications, advantages and limitations. *Expert Systems with Applications* 2024;242:122807.
147. Seibold C, Künzel J, Hilsmann A, and Eisert P. From explanations to segmentation: using explainable AI for image segmentation. arXiv preprint arXiv:2202.00315 2022.
148. USDA APHIS. ID Tools - Interactive Identification Tools. Accessed: 2025-03-16. 2025. URL: <https://idtools.org/identify.cfm?sort=dateDesc>.
149. Genze N, Vahl WK, Groth J, Wirth M, Grieb M, and Grimm DG. Manually annotated and curated Dataset of diverse Weed Species in Maize and Sorghum for Computer Vision. *Scientific Data* 2024;11:109.

150. Steininger D, Trondl A, Croonen G, Simon J, and Widhalm V. The cropandweed dataset: A multi-modal learning approach for efficient crop and weed manipulation. In: *Proceedings of the IEEE/CVF Winter Conference on Applications of Computer Vision*. 2023:3729–38.
151. Wang P, Tang Y, Luo F, et al. Weed25: A deep learning dataset for weed identification. *Frontiers in Plant Science* 2022;13:1053329.
152. Santos Ferreira A dos, Freitas DM, Silva GG da, Pistori H, and Folhes MT. Weed detection in soybean crops using ConvNets. *Computers and Electronics in Agriculture* 2017;143:314–24.